



TFM

Control of Voltage Source Converters connected to Low-Inertia Power systems

Author: Pedro Sánchez Bas

Directors:

Francisco Javier Renedo Anglada

Agustí Egea Álvarez



Declaro, bajo mi responsabilidad, que el Proyecto presentado con el título
Control of Voltage Source Converters connected to Low-Inertia Power
Systems

en la ETS de Ingeniería - ICAI de la Universidad Pontificia Comillas en el
curso académico 2019/2020 es de mi autoría, original e inédito y
no ha sido presentado con anterioridad a otros efectos. El Proyecto no es
plagio de otro, ni total ni parcialmente y la información que ha sido tomada
de otros documentos está debidamente referenciada.

Fdo.: Pedro Sánchez Bas

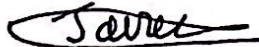
Fecha: 7/7/2020



Autorizada la entrega del proyecto

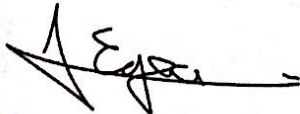
EL DIRECTOR DEL PROYECTO

Fdo.: Francisco Javier Renedo, Anglada Fecha: 7-7-2020



Fdo. Agustí Egea Álvarez

Fecha: 7-7-2020



CONTROL DE CONVERTIDORES VSC CONECTADOS A REDES DE BAJA INERCIA

Autor: Sánchez Bas, Pedro

Director: Francisco Javier Renedo Anglada

Entidad colaboradora: ICAI – Universidad Pontificia Comillas

Resumen:

Las recientes décadas en el panorama de la ingeniería eléctrica se han caracterizado por la progresiva introducción de energías renovables, principalmente solar FV y eólica, en el parque de generación de energía eléctrica. Esto ha conllevado la sustitución de generación convencional, llevada a cabo a través de máquinas síncronas, por generación a través de convertidores de electrónica de potencia.

La generación de energía con estos dispositivos ha supuesto, entre otros, el desafío tecnológico que es objeto de estudio de este Trabajo de Fin de Máster: el control de convertidores VSC (Voltage Source Converter) conectados a redes de baja inercia, es decir, redes en las cuales el peso de los generadores síncronos es pequeño en comparación con el de la generación a través de convertidores de electrónica de potencia.

Podemos definir la inercia como la propiedad de las redes eléctricas AC de mantener su frecuencia antes perturbaciones en la demanda u otros eventos. La siguiente ecuación describe matemáticamente la relación entre inercia, frecuencia y el equilibrio entre generación y demanda:

$$H \frac{df}{dt} = P_{generada} - P_{demandada}$$

A día de hoy existen una serie de esquemas de control de convertidores que configuran el estado del arte. La configuración más típica para controlar un VSC es la conocida como “grid following” que consiste en una medida de la frecuencia de la red, a la cual el convertidor imita, y calcula su tensión de salida para que esté acorde con esta. De esta configuración cabe destacar que la aportación de inercia a la red es nula. El esquema de control se ofrece a continuación:

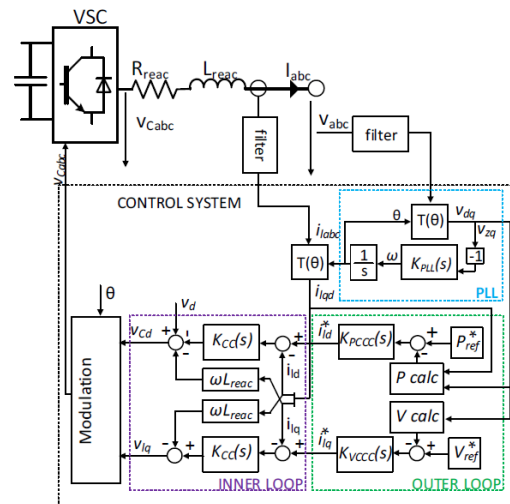


Figura 1: Esquema del control “grid following”

Como se aprecia en este esquema de control existe una primera etapa de medición de la frecuencia de la red y un posterior control en cascada para controlar potencia activa y tensión en el punto de conexión.

Por otro lado, la configuración de máquina síncrona virtual, a diferencia del “grid following” tiene una serie de

términos en la potencia de salida asociados a la frecuencia de la red, por lo que puede aportar una cierta inercia de forma virtual.

Este trabajo tiene como objetivos principales:

- Realizar un análisis exhaustivo de las redes de baja inercia y los problemas tecnológicos y soluciones propuestas a día de hoy
- Realizar un análisis de las principales configuraciones de control de VSC
- Simular un control de tipo “grid following” conectado a red de baja inercia y analizar las implicaciones que tiene esto en el control del convertidor

Como herramientas de trabajo se usa el entorno de simulación de Matlab/Simulink, apoyado por la herramienta de SymPowerSystems, una toolbox de Matlab destinada a simular sistemas eléctricos con elevado grado de precisión.

Después de llevar a cabo las simulaciones se obtienen una serie de resultados. Uno de los más significativos se puede concretar en la siguiente gráfica:

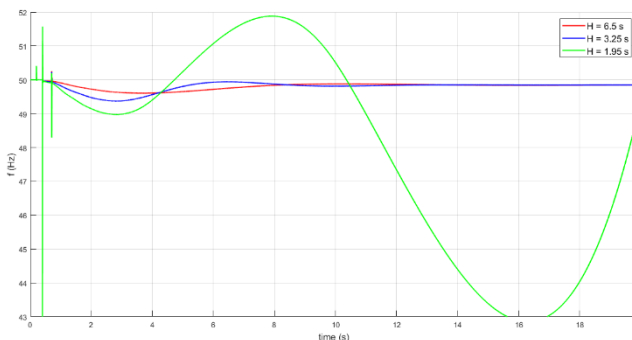


Figura 2: Resultados gráficos

Esta gráfica se corresponde con el resultado de una simulación en la que se va reduciendo la cantidad de inercia en la red, y en ella se observa que se llega a producir una situación de inestabilidad a partir de cierto nivel de inercia.

Como conclusiones principales del proyecto se tiene que:

- A medida que se reduce la inercia total del sistema la estabilidad de frecuencia se ve comprometida
- Se observa que en el caso estudiado el control del convertidor VSC no se ve afectado por la cantidad de inercia de la red

CONTROL OF VSC CONNECTED TO LOW INERTIA POWER SYSTEMS

Author: Sánchez Bas, Pedro

Director: Francisco Javier Renedo Anglada

Entity: ICAI – Universidad Pontificia Comillas

Abstract:

The most recent decades in electrical engineering have been characterized by the progressive introduction of renewable energies, mostly solar PV and wind, into the structure of generation of electric power. This has been translated into the substitution of traditional synchronous generation to generation through power electronics converter devices.

The generation of electric power with such devices has meant, along with others, the technological challenge that this document faces: the control of VSC (Voltage source converters) connected to low inertia grids, this is, electric grids where the weight of traditional synchronous generation is low compared to converter generation.

We can define inertia as the property of power systems that allows them to tend to maintain their frequency over frequency-related events, such as imbalances between generation and demand and others. The following equation describes the relation between frequency, inertia and imbalances between generation and demand:

$$H \frac{df}{dt} = P_{generated} - P_{demanded}$$

Nowadays, there are a series of control schemes in the state of the art of VSC. The most common configuration is known as grid following structure, which consists in measuring grid frequency and providing an output voltage at this exact frequency. From this configuration the most important characteristic is the fact that there is no inertia provided to grid by the converter. The control scheme is provided in the following figure:

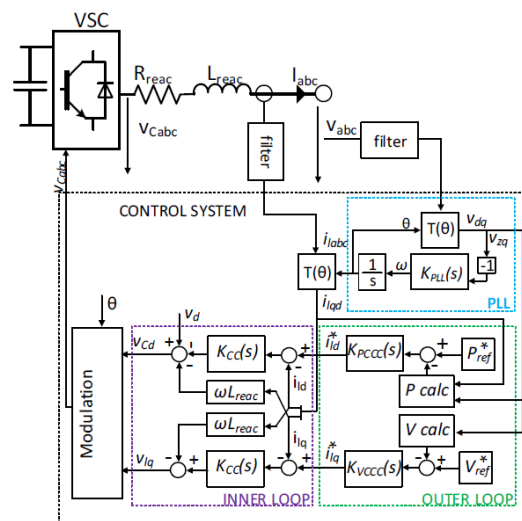


Figure 1: Grid following control scheme

As we can see in this scheme there is a PLL, which measures frequency and a cascade control loop for controlling both voltage and the connection point and active power injection.

In the other hand, virtual synchronous machines provide an output power which depends on grid frequency, allowing them to provide some virtual inertia to the power system.

The most important tasks for this TFM are:

- Analyzing low inertia grids and state of the art of solutions regarding low inertia
- Analysis of the most relevant configurations of VSC
- Simulating a grid following control connected to a low inertia power system

The tool used for this project is the simulation environment provided by matlab/Simulink, with the SymPowerSystems toolbox.

After performing some simulations we reach graphical results such as the following:

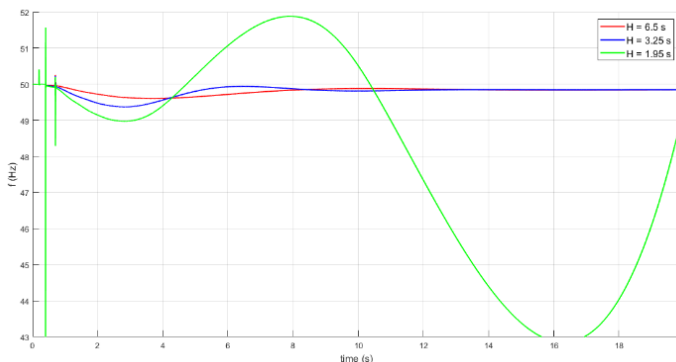


Figure 2: Graphical results

This graph corresponds to a simulation where the amount of inertia is decreasing. We can see that, at a certain limit instability is reached

when the total amount of inertia is low.

The most relevant conclusions extracted from this project are:

- As the total amount of inertia in the grid decreases frequency stability is compromised, even reaching unstable scenarios
- In this particular case of study the control of the VSC converters is not compromised by the amount of inertia in the grid



TFM

Control of Voltage Source Converters connected to Low-Inertia Power systems

Author: Pedro Sánchez Bas

Directors:

Francisco Javier Renedo Anglada

Agustí Egea Álvarez





Index

1.	Introduction	4
1.1	State of the art.....	6
1.2	Project scope.....	8
1.3	Document organization.....	9
2.	Modeling and control of VSC converters.....	10
2.1	Park transformation	11
2.2	Current control	13
2.1.1	PLL.....	14
2.1.2	Outer loop.....	15
2.1.3	Inner loop	16
2.3	Voltage control.....	19
3.	VSC connected to infinite grid	20
4.	Low inertia power systems connected to VSC.....	25
4.1	Mathematical modeling.....	25
4.1.1	Inertia.....	25
4.1.2	Stability	26
4.2	Low inertia power systems.....	29
4.3	Case of study	33
5.	Simulation of Voltage Source Converters connected to Low inertia power systems	35
5.1	Scenario 1: Changing the value of H	35
5.2	Scenario 2: Changing the nominal power.....	40
5.3	Conclusions	44
6.	Conclusions and future work.....	45
7.	Annex	47
7.1	System parameters	47
7.2	Budget	50
7.3	Sustainable Development Goals.....	51
8.	Acknowledgments.....	53
9.	References.....	54

Figure index

Figure 1: VSC model [5].....	5
Figure 2: Visual representation for RoCoF [7]	5
Figure 3: Model representation of VSC.....	10
Figure 4: Clarke transformation.....	11
Figure 5: PLL basic structure	14
Figure 6: Current control outer loop.....	15
Figure 7: Connection between grid and VSC.....	16
Figure 8: Current control inner loop.....	17
Figure 9: PI control structure.....	18
Figure 10: Voltage control structure	19
Figure 11: Infinite grid model.....	20
Figure 12: Simulink model of the infinite grid	20
Figure 13: Simulink model overview.....	21
Figure 14: Ps. Step in Ps ref (infinite grid).....	22
Figure 15: Qs. Step in Ps (infinite grid)	22
Figure 16: Ps. Step in Qs (infinite grid)	23
Figure 17: Qs. Step in Qs (infinite grid).....	23
Figure 18: Frequency dynamics block diagram.....	27
Figure 19: Complete block diagram.....	27
Figure 20: Share of renewables in the UK [12]	29
Figure 21: Dynamic differences regarding inertia in the UK [13]	30
Figure 22: Distribution of offshore wind generation in the UK [14]	30
Figure 23: Share of renewables in the nordic grid [15].....	31
Figure 24: Kundur power system.....	33
Figure 25: Low inertia case study power system.....	33
Figure 26: Simulink model of the low inertia power system.....	34
Figure 27: Frequency plot for scenario 1	36
Figure 28: Active power plot for scenario 1	36
Figure 29: Active power plot for scenario 1, detailed	37
Figure 30: Reactive power plot for scenario 1	37
Figure 31: Reactive power plot for scenario 1, detailed.....	38
Figure 32: Voltage plot for scenario 1.....	38
Figure 33: Frequency plot for scenario 2	40
Figure 34: Active power plot for scenario 2	41
Figure 35: Active power plot, scenario 2, detailed	41
Figure 36: Reactive power plot for scenario 2	42
Figure 37: Reactive power plot, scenario 2, detailed.....	42
Figure 38: Voltage plot for scenario 2.....	43
Figure 39: Low inertia power system elements	47
Figure 40: SDG.....	51

1. Introduction

The last few decades have witnessed an unprecedented change in power systems, with the progressive development and implementation of renewable energies, in order to replace fossil fuel-based generation. As an example, in wind generation 60.4 GW of energy capacity was installed globally in 2019, a 19 per cent increase from installations in 2018 and the second-best year for wind historically [1]. Also, solar energy generation is growing rapidly, with forecasts from the International Energy Agency that predict that between 2019 and 2024 solar PV accounts for almost 60 % of the total expected growth in renewable energies [2].

This growth implies many technological challenges and issues to be solved in order to maintain a high-quality service. Some of these problems are already relevant nowadays, especially in small and isolated electrical power grids. In this MSc dissertation it is intended to focus into the analysis of one these technological challenges: Low Inertia Power Grids.

Here are a few examples of power systems with problems regarding Inertia:

- Texas electric power system (ERCOT) has 15 % of its energy coverage from wind energy, which can reach up to 45 % of instantaneous power. Known to be one of the most competitive markets, it has already come up with some market-based solutions to maintain system inertia within controlled limits [3]
- The UK power system has increased its renewable energy capability, reaching a 36 % of renewable share of generation. Although it's got an interconnection with central Europe, it is highly isolated and faces many problems regarding system stability

Classical power generation systems are based on one basic electromagnetic principle: transforming the energy of a rotating element into electrical energy through magnetic induction. These generators are called synchronous generators because they spin at a fixed frequency, which is the same as the generator rotational speed (in AC grids, which are the ones this document will focus on). This principle is fundamental in order to control the balance between power generation and demand.

We can define inertia as the resistance of any rotating object to change its angular speed. Because of synchronous generators spin at the grid frequency we can express the inertia of a generator as the resistance to change the grid frequency. Instead of physical forces trying to stop generators from spinning, the opposition to generators speed is an increase in the total power demand in the network. This implies that an increment of power supplied by the generator will increase the frequency. The following equation illustrates the behavior of frequency as a function of power supplied and demanded (H stands for inertia):

$$H \frac{df}{dt} = P_{generated} - P_{demanded} \quad (Ec. 1)$$

Where $P_{generated}$ stands for total generated power, $P_{demanded}$ the total power consumption and f the grid frequency.

In modern electrical systems synchronous generators make the majority of total power generation, but the share of renewables is considerable and rapidly increasing. Renewable energies are introduced into the network through power electronics converters. These converters can be modeled as AC voltage sources, which will give us some degrees of freedom to control the most important parameters: active and reactive power injection into the grid [4]. But they also lack one of the most important characteristics of synchronous generators: they are not synchronized with grid frequency. The following image shows the basic VSC (Voltage Source Converter) model:

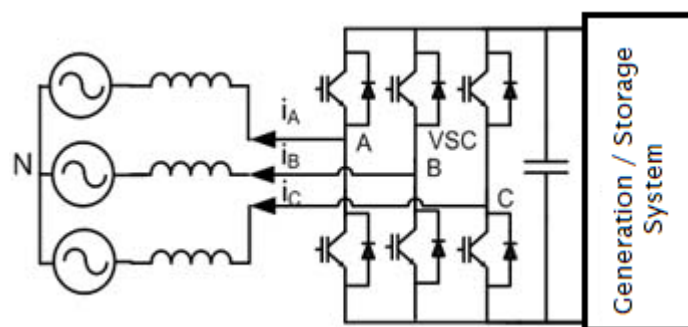


Figure 1: VSC model [5]

The Generation/Storage system in the right could either be a battery or a DC source, which could represent DC current coming from a solar panel or from a wind turbine (after an AC/DC conversion stage). On the left side, the 3 voltage sources represent a 3-phase grid.

One of the most important parameters required to study system stability is RoCoF (Rate of Change of Frequency). RoCoF determines the dynamics of frequency: changes in this rate can lead to many system failures such as a low power quality or false control actions [6]. There are many challenges nowadays relating RoCoF measurement and control, especially when it comes to identifying waveform patterns in order to achieve a better understanding of the failure cause. The following image illustrates the relation between RoCoF and Inertia:

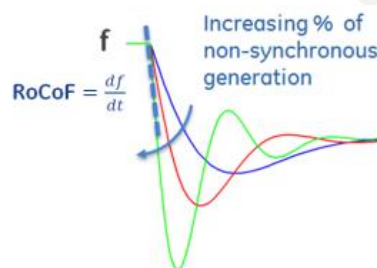


Figure 2: Visual representation for RoCoF [7]

In the graph the blue function stands for more synchronous generation, while red and green, respectively, stand for less synchronous generation. It is clear that the more non-synchronous generation, the more unstable the frequency waveform is (note that the graph represents frequency over time). More synchronous generation is equal to less system Inertia; therefore, we can establish an inverse relation between RoCoF and Inertia.

As it was mentioned before, the share of renewable energies in the electric market has grown rapidly in the last few years and will continue to do so in the next decades. The fact that these energy sources are coupled to the grid through power electronic converters has crucial implications in the grid: total inertia decreases as more power electronics converters are used for power generation.

This dissertation will focus on studying low inertia grids, specially on how to control VSC (Voltage Source Converters) in order to reduce the critical effect of low inertia in power systems. Because of the constant increase of renewable energies share, power converters could be dominating generation in most power systems in the future.

1.1 State of the art

Nowadays there are currently 2 main power converter philosophies: Current Controlled VSC, or grid following, and Voltage Control VSC, or grid forming. The difference between them relies on frequency control: Current controlled power converters measure the grid frequency and output a voltage signal with that specific frequency, while Voltage controlled VSC power converters fix the grid frequency. They both have two degrees of freedom when it comes to controlling output voltage: the signal phase and the signal amplitude. Phase will influence active power flows while voltage will be used to control reactive power flow.

- Current controlled VSC

VSC stands for Voltage Source Converter, which implies that the equivalent model of the power converter is an ideal voltage source. As mentioned before, this control structure tries to follow the grid frequency. Generally, this type of VSC controls:

- Active Power injection into the grid
- Reactive Power injection or voltage

The most common approach is using the so-called vector control, in which the converter synchronises with the voltage of the connection point (details of the controllers will be described in the project). In other words, current-controlled VSCs need an active grid to be connected to. For this reason, current-controlled VSCs are also commonly called “grid following” VSCs. Current renewable generators such as wind turbines or solar photovoltaic (PV) generators use current-controlled VSCs. The following diagram illustrates the control structure:

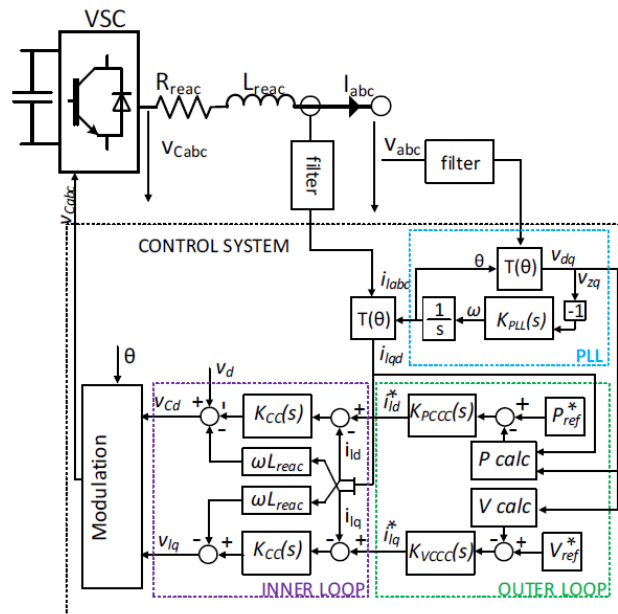


Fig. 3: Current Control structure [8]

- Voltage Controlled VSC

In this structure the following variables are controlled:

- Output frequency
- The magnitude of the voltage at connection point

This implies that a voltage controlled VSC could supply a passive load, for example. In other words, it could create a grid itself. For this reason, voltage controlled VSCs are also commonly called “grid forming” VSCs. One of the most relevant applications of this type of control of the VSCs for future power systems is when dealing with power systems with large amounts of non-synchronous generation. However, there are still challenges in the operation of power systems with a large number of grid forming VSCs. The following diagram shows the control structure:

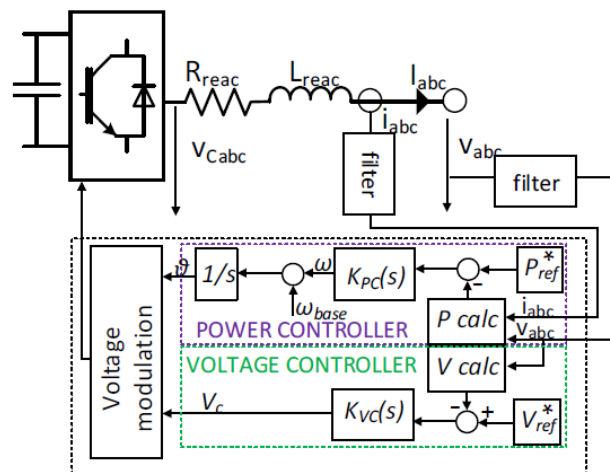


Fig. 4: Virtual Synchronous Machine control structure [9]

A specific configuration of these controllers can allow us to emulate the behavior of a synchronous machine using a power electronics converter, they are called Virtual Synchronous Machines. VSM are based on standard power converters with an energy storage. This storage provides the synchronous-like functionality, changing the power flow accordingly when frequency changes, as the following equation states:

$$P_{VSG} = P_0 + K_I \frac{d\Delta\omega}{dt} + K_P \Delta\omega \quad (Ec. 2)$$

In this equation the term on the left, P_{VSG} , stands for total output power, which is the sum of converter active power reference, P_0 , plus a term proportional to the derivative of the frequency, $K_I \frac{d\Delta\omega}{dt}$, (which emulates the natural response of any synchronous machine), and the last term in the right, $K_P \Delta\omega$, which represents primary control. K_I stands for the inertia parameter ($2H$, where H is the inertia), and K_P is proportionally related to primary control gain. The following image describes a VSM:

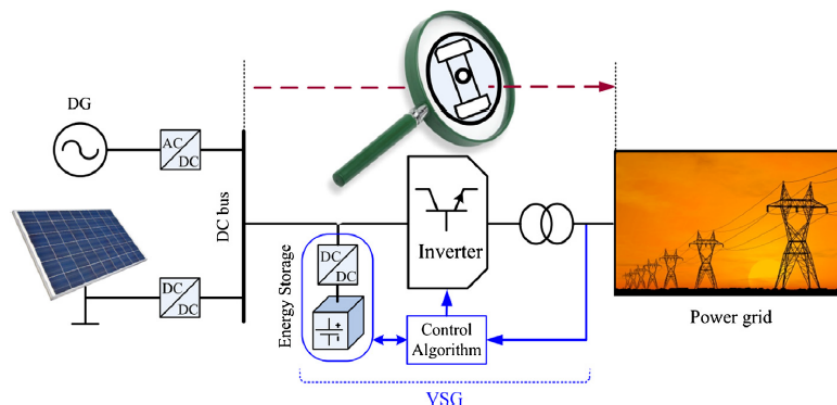


Fig. 5: Basic VSM structure [10]

1.2 Project scope

The scope of this work can be summarized in the following objectives:

- Perform an extent analysis on Low Inertia Power Systems: defining system inertia, recent problems relating RoCoF and the general evolution of power systems until current topology
- Analysis of electronic power converters functioning, and most relevant configurations used nowadays
- Analysis of VSC control when specifically connected to a low inertia power system



1.3 Document organization

This document is organized in order to show the evolution from the simplest model, progressively adding new elements and complexity. This makes the process of understanding the role of every block much simpler and intuitive.

First, a brief explanation of VSC and the main control approaches will be provided. In this chapter some information about the case of study's grid will be presented. After this chapter we will perform simulations on different control schemes in order to extract conclusions.

The first model is the current control converter connected to an infinite grid. This is the simplest case since the infinite grid acts as an ideal voltage source. Later on, some complexity will be added to the infinite grid (basically a connection impedance).

After analyzing some results, the second model will be the same current control converter connected to a low inertia grid. In this model we will analyze the effect of inertia on the most important performance measures.

Finally, some general conclusions will be presented, regarding all the topics involved in this MSc dissertation.



2. Modeling and control of VSC converters

VSC stands for Voltage Source Converter. This term is used to refer to power electronics converters which are used to transform a DC current into a grid-compatible AC current. It is the most common tool used to inject power from renewable energies into an electric power system, but it also presents many other applications.

According to the VSC basic structure, which is presented in Figure 1, we can model one side of the VSC as a DC power bus. The converter consists on several electrical switches (IGBT transistors) [ref] that provide a specific time function which outputs an AC voltage on the other side of the converter. The “raw” AC voltage is a basic square wave, but because of the presence of filtering elements, both in the grid and the VSC we can consider the output signal to be purely sinusoidal, therefore an **ideal AC voltage source** from the perspective of the grid.

From now on the following schematics will be used in order to represent a VSC:

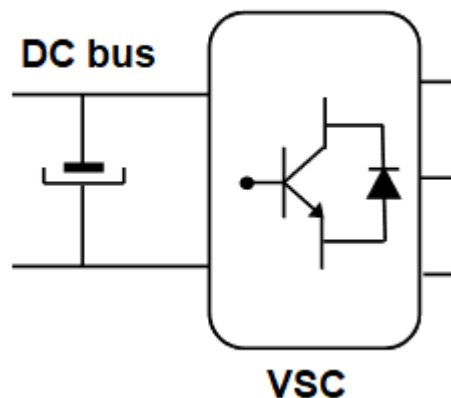


Figure 3: Model representation of VSC

As mentioned before, the main use of VSC is to convert DC power from renewables into an AC grid. The converter acts as an ideal source that injects both active and reactive power. The variable used to control this injection is the output voltage, which can be splatted into two control variables: amplitude (or module), and phase. For some control configurations the frequency is also a control variable, but for our purpose we will suppose that it is fixed by grid. The VSC control configuration basically determines how the power injection is related to the output voltage through a closed feedback loop [11]. In this chapter a brief explanation of those configurations will be given.

2.1 Park transformation

In this chapter a brief explanation of the Park transformation used in this project will be given. The Park transformation is commonly used in 3-phase power systems in order to reduce the number of variables taken into account, and to simplify control and regulation of any of those variables.

Given a certain 3-phase power system any variable $f(t)$ consists in 3 components: $f_a(t)$, $f_b(t)$ and $f_c(t)$. Given these 3 components we define the space vector as the following complex variable:

$$\vec{f}(t) = k_1 \left(e^{j0} f_a(t) + e^{\frac{2\pi}{3}j} f_b(t) + e^{-\frac{2\pi}{3}j} f_c(t) \right) \quad (Ec. 3)$$

The complex number represented by $\vec{f}(t)$ can be decomposed into a real and imaginary component as follows:

$$\vec{f} = f_\alpha + jf_\beta \quad (Ec. 4)$$

Where f_α and f_β are called the α - β components of the variable \vec{f} . With this transformation, called Clarke transformation, we can analyze the behavior of any variable just by looking at its α - β components, which can be seen as the projection of the $\vec{f}(t)$ vector into some perpendicular α - β axes. The following image illustrates this idea:

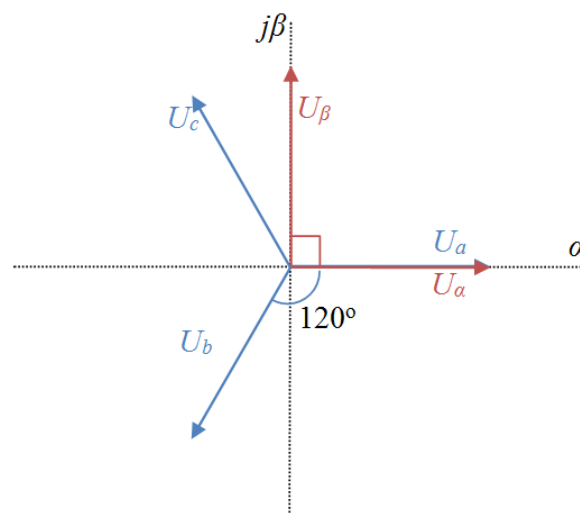


Figure 4: Clarke transformation

The problem with this transformation is that sinusoidal functions will remain sinusoidal after the transformation. From the control point of view it's very useful to

transform those sinusoidal functions into variables that tend to be constant over time. The Park transformation also projects the $\vec{f}(t)$ vector into a pair of perpendicular axes, but those axes rotate at the frequency of the power system. This implies that in a stable situation, any 3-phase variable can be represented through constant components. The Park transformation can be expressed as:

$$\vec{f}_{dq}(t) = k_1 \left(e^{-j\theta} f_a(t) + e^{-j(\theta - \frac{2\pi}{3})} f_b(t) + e^{-j(\theta + \frac{2\pi}{3})} f_c(t) \right) \quad (Ec.5)$$

Where k_2 is constant, real value and \vec{f}_{dq} is a complex number which can also be decomposed in 2 components the following way:

$$\vec{f}_{dq}(t) = f_d + jf_q \quad (Ec.6)$$

For the complete expression of the space vector in terms of the Park transformation a third component is required. This is called the homopolar component and it can be calculated through the following formula:

$$f_0 = k_2(f_a + f_b + f_c) \quad (Ec.7)$$

Where k_2 is constant, real value. Note that in any case of equilibrium in a 3-phase network, this is, the same current in every one of the 3 wires, the homopolar component will be 0. For this reason, f_0 is quite often ignored when analyzing generic power systems. Taking all the terms into account we can express the Park transformation as a linear transformation between two vectors, expressed through the following matrix:

$$\begin{bmatrix} f_0 \\ f_d \\ f_q \end{bmatrix} = \begin{bmatrix} k_2 & k_2 & k_2 \\ k_1 \cos(\theta) & k_1 \cos\left(\theta - \frac{2\pi}{3}\right) & k_1 \cos\left(\theta + \frac{2\pi}{3}\right) \\ -k_1 \sin(\theta) & -k_1 \sin\left(\theta - \frac{2\pi}{3}\right) & -k_1 \sin\left(\theta + \frac{2\pi}{3}\right) \end{bmatrix} \begin{bmatrix} f_a \\ f_b \\ f_c \end{bmatrix} \quad (Ec.8)$$

Where θ verifies:

$$\frac{d\theta}{dt} = f_{grid} \quad (Ec.9)$$

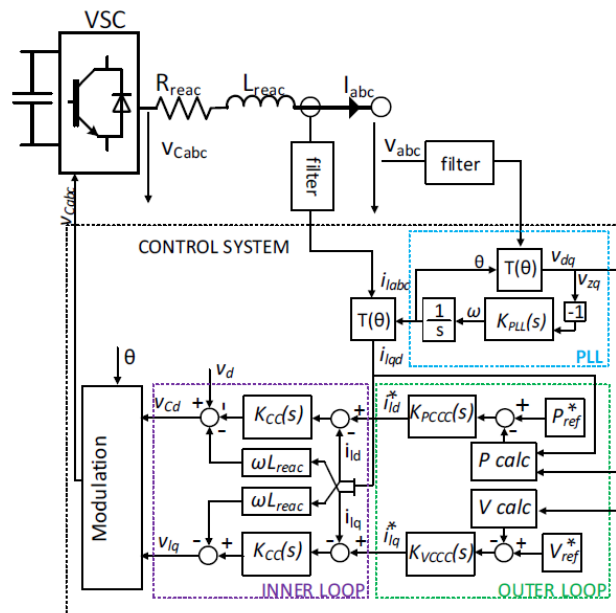
Given all the possible values of k_1 and k_2 there are infinitely many transformations. In practice there are very few ones that are commonly used, each one with its unique properties. The transformation that is used for this project is called the power invariant one, because the expressions of active and reactive power can be obtained

directly from the values of voltage and current, without any other added terms. From now on the values for k_1 and k_2 will be fixed to the following:

$$k_1 = \sqrt{\frac{2}{3}} \quad \text{and} \quad k_2 = \sqrt{\frac{1}{3}}$$

2.2 Current control

This control configuration is also referred as grid-following. The main idea behind this structure is that the output voltage “follows” the grid frequency. The way that this control follows the grid frequency is by measuring the phase of the grid voltage through a PLL (Phase locked loop, which is explained further in this chapter) and using this phase to calculate the output voltage. Going back to the control scheme provided in chapter one we can see 3 main components in this structure:



The main components of the control system are the PLL and the outer and inner control loops. The PLL measures the grid voltage and provides the phase needed for the Park transformation, $T(\theta)$. The outer loop transforms the active power and voltage references into i_d and i_q references for the inner loop, which provides the necessary output voltage command. This command goes onto the modulator stage, which controls the switching function of the transistors.

The typical configuration controls both the active and reactive power injection, but just as we can see in this particular example the reactive power injection can be substituted by the voltage (module) of the grid at the connection point.

2.1.1 PLL

PLL stands for Phase locked loop. It is a closed loop control system in which the output variable is the phase of the grid. In terms of d-q axis the equivalent to following the grid frequency is to set the d axis to have the same angle as the grid voltage. Therefore, the q component of the grid voltage must be equal to zero all the time in order for the PLL to work properly. The following scheme illustrates the control structure:

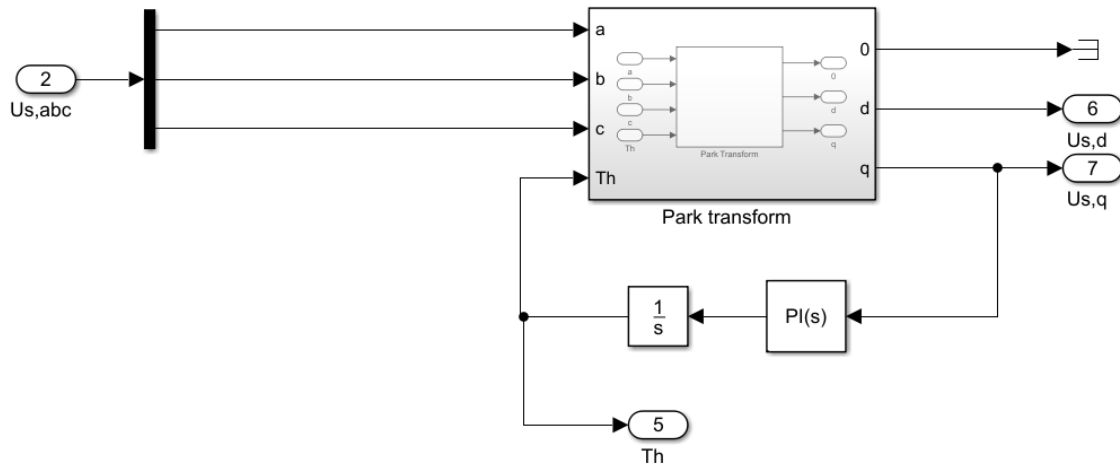


Figure 5: PLL basic structure

The control can be summarized into a PI control where the input is the q component of the grid voltage. Because of the integrator in the PI control, in steady state conditions and if the system is stable $u_{s,q}$ must eventually be zero ($\overline{U_s}$ stands for grid voltage). The variable that makes $u_{s,q}$ go to zero is the input of the Park transformation, therefore the phase (Th stands for Theta) of the grid voltage. The dynamics of this control are much faster than any other control dynamics (inner and outer loop), therefore they can be considered almost instantaneous for the VSC.

Mathematically, the PLL can be modeled considering that $u_{s,q}$ is the projection of $\overline{U_s}$ into the q axis, by the following equation:

$$u_{s,q} = |\overline{U_s}| \sin(\omega_0 t - \theta_p + \theta_0) \quad (Ec. 10)$$

If the PLL works, then $u_{s,q} \approx 0$ and $\sin(\omega_0 t - \theta_p + \theta_0) \approx 0$. Therefore, the sine function can be substituted by its input, leaving the following equation:

$$\frac{u_{s,q}}{|\overline{U_s}|} = \omega_0 t - \theta_p + \theta_0 \quad (Ec. 11)$$

Rewriting θ_p as the integral over time of $\omega(t)$ we reach the final expression that describes the behavior of the PLL:

$$\frac{u_{s,q}}{|U_s|} = \omega_0 t - \int \omega(t) dt + \theta_0 \quad (Ec. 12)$$

This equation summarizes the structure of the PLL as presented in Figure 5.

2.1.2 Outer loop

Taken that the Park transformation is the already presented one we can derive the expressions that relate P and Q with voltage and current in d-q terms:

$$\bar{S}_s = p_s + jq_s = \overline{U_{dq} I_{dq}^*} = (u_{s,d} + ju_{s,q})(i_d - ji_q) \quad (Ec. 13)$$

$$p_s = u_{s,d}i_d + u_{s,q}i_q \quad (Ec. 14)$$

$$q_s = u_{s,q}i_d - u_{s,d}i_q \quad (Ec. 15)$$

If we take into account that $u_q = 0$ and express both currents as a function of other terms:

$$i_{d\ ref} = \frac{p_{ref}}{u_d} \quad i_{q\ ref} = \frac{-q_{ref}}{u_d}$$

Therefore, the outer loop calculates the current reference for the inner loop as a function of grid voltage and active and reactive power references. It is common to find a PI control in series with this calculation, but it is not the case of this dissertation. The following scheme represents the Simulink implementation of the outer loop:

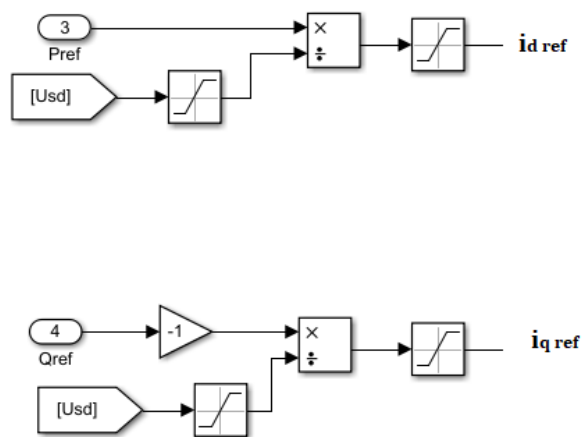


Figure 6: Current control outer loop

2.1.3 Inner loop

The aim of the inner loop is to calculate the output voltage required to control $i_{d\text{ref}}$ and $i_{q\text{ref}}$. In order to understand this control loop, we must derive the expression of the transfer function between both currents and the d-q output voltage. We start with the electrical model of the connection between grid and converter:

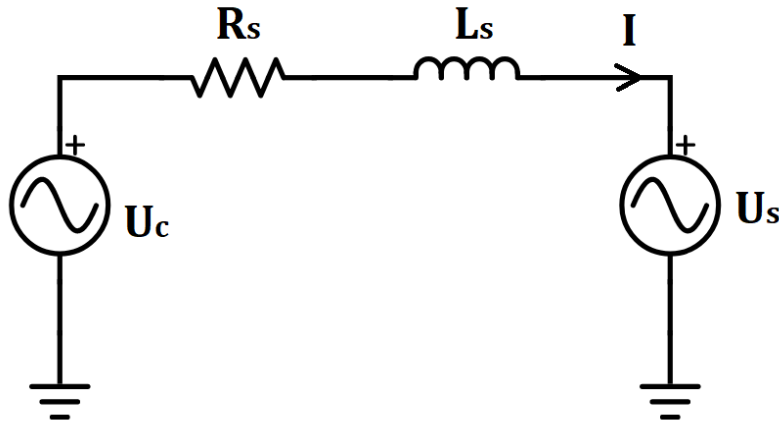


Figure 7: Connection between grid and VSC

U_c stands for converter voltage, U_s for grid voltage and R_s and L_s for resistance and inductance of the connection line. If we apply KVL we can derive the expression that relates U_c and U_s :

$$\bar{U}_c = R_s \bar{I} + L_s \frac{d\bar{I}}{dt} + \bar{U}_s \quad (\text{Ec. 16})$$

If we apply the Park transform to both sides of the equation and separate d and q components we come up with the following expression:

$$u_{c,d} = R_s i_d - L_s \omega i_q + L_s \frac{di_d}{dt} + u_{s,d} \quad (\text{Ec. 17})$$

$$u_{c,q} = R_s i_q + L_s \omega i_d + L_s \frac{di_q}{dt} + u_{s,q} \quad (\text{Ec. 18})$$

Note that the homopolar component has been ignored (we will work with the equilibrated load hypothesis). If we apply the Laplace transform in both sides of the equations, we reach the dynamic relation between currents and voltages (also considering that $u_{s,q} = 0$):

$$u_{c,d}(s) = (R_s + L_s s) i_d(s) - L_s i_q(s) + u_{s,d}(s) \quad (\text{Ec. 19})$$

$$u_{c,q}(s) = (R_s + L_s s) i_q(s) + L_s i_d(s) \quad (\text{Ec. 20})$$

If we rearrange the terms to set $i_d(s)$ and $i_q(s)$ as a function of the other variables:

$$i_d(s) = \frac{1}{R_s + L_s s} u_{c,d}'(s) \quad i_q(s) = \frac{1}{R_s + L_s s} u_{c,q}'(s)$$

Where

$$u_{c,d}'(s) = u_{c,d}(s) + L_s i_q(s) - u_{s,d}(s) \quad u_{c,q}'(s) = u_{c,q}(s) - L_s i_d(s)$$

$u_{c,d}'(s)$ and $u_{c,q}'(s)$ are called virtual command signals since they don't represent the converter voltage itself, but with some other terms that we will include in the control model. Note that the transfer function between input and output is the same for d and q, and that there are a couple of crossed terms (i_q with $u_{c,d}'$ and i_d with $u_{c,q}'$). We can use this transfer function to design a PID control and implement it for the inner loop. Nevertheless, we have to take into account both crossed terms and the expression of the virtual command in order to calculate $u_{c,d}$ and $u_{c,q}$. The following scheme represents the inner loop taking into account all these:

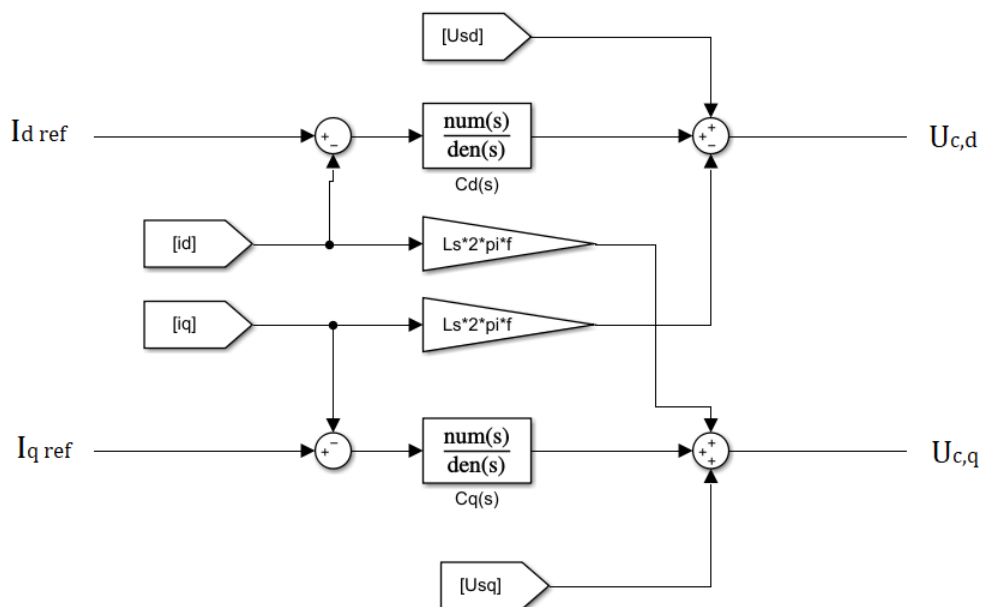


Figure 8: Current control inner loop

The control design consists in choosing $C_d(s)$ and $C_q(s)$ in order to achieve a stable closed-loop system maintaining an optimal performance in terms of following the reference values for active and reactive power (or voltage). For both d and q controls a PI model is considered. The structure of a PI control is the following:

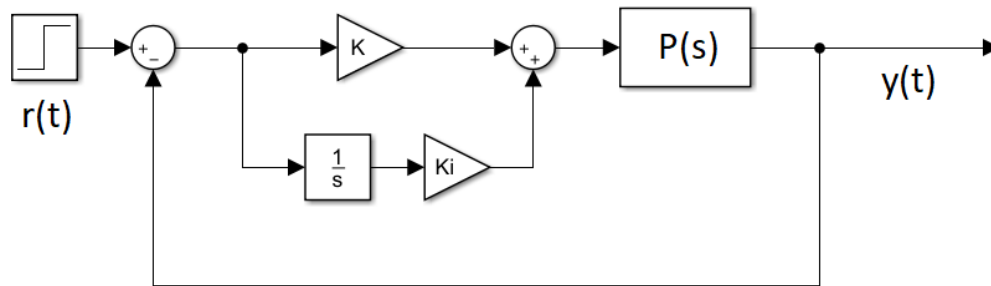


Figure 9: PI control structure

Where $r(t)$, is the reference, $P(s)$ is the plant, and $y(t)$ is the output (controlled variable). In our case, the plant is the same for both d and q axis:

$$P(s) = \frac{1}{R_s + L_s s}$$

Taking into account the presented control structure the closed loop system will have the following transfer function:

$$F(s) = \frac{C(s)P(s)}{1 + C(s)P(s)} = \frac{\frac{K}{L_s}s + \frac{K_i}{L_s}}{s^2 + \frac{R_s + K}{L_s}s + \frac{K_i}{L_s}} \quad (Ec. 21)$$

This remaining transfer function establishes the relation between $r(t)$ and both $id(t)$ and $iq(t)$ (same transfer function for both variables). We can see that $F(s)$ is a second order transfer function, therefore we will organize the terms in the denominator to choose the damping and natural frequency, with the following equality:

$$F(s) = \frac{K(1 + \tau s)}{s^2 + 2\zeta\omega_n s + \omega_n^2} = \frac{\frac{K}{L_s}s + \frac{K_i}{L_s}}{s^2 + \frac{R_s + K}{L_s}s + \frac{K_i}{L_s}} \quad (Ec. 22)$$

Because of the 2 control parameters there are 2 degrees of freedom for control design, which will be used to fix ζ and ω_n . By solving Ec.22, we can see the values required for K_i and K :

$$K_i = \omega_n^2 L_s$$

$$K = 2\zeta\omega_n L_s - R_s$$

Typical values for ζ are in the range of 0,7 and higher, while ω_n is chosen to be faster than the fastest dynamics of the plant we want to control. In this case ω_n is fixed at a value 10 times higher than the grid frequency.

2.3 Voltage control

Also known as “grid forming”, this control strategy differs from the current control in the fact that voltage controlled VSC provide their own frequency orientation. This means that the controller does not measure the frequency in the grid, but rather is the frequency reference in the grid itself. As well as in the current control structure the 2 available degrees of freedom (Angle and Voltage module) allow to control to variables, which are typically voltage in the connection point and active power injection. The following figure shows the structure of this control strategy:

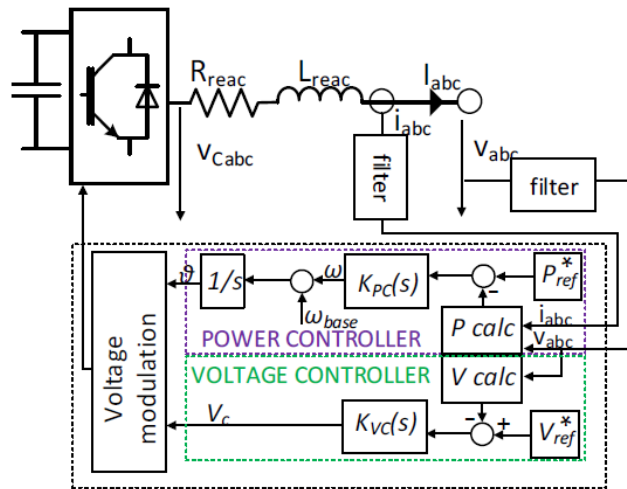


Figure 10: Voltage control structure

As it is shown in the image, there are 2 parallel control systems, which provide one variable each to the voltage modulation stage. Note that the output from the outer loop in the power controller is a frequency value, which is then compared to the base value of the frequency (nominal value chosen for the grid).

In this document all the simulations and the theoretical work is focused mainly in the current control structure, as it is the most common nowadays for non-synchronous power generation, nevertheless there is a growing interest in this particular type of VSC control as it could solve many of the problems regarding low inertia in electrical grids in a near future.

3. VSC connected to infinite grid

In this chapter we will analyze and simulate the simplest electrical model for the grid: an infinite grid model. In this case the grid is substituted with an ideal AC voltage source, with a constant voltage. Figure 6, used to describe the inner loop for the current control, illustrates the model behavior:

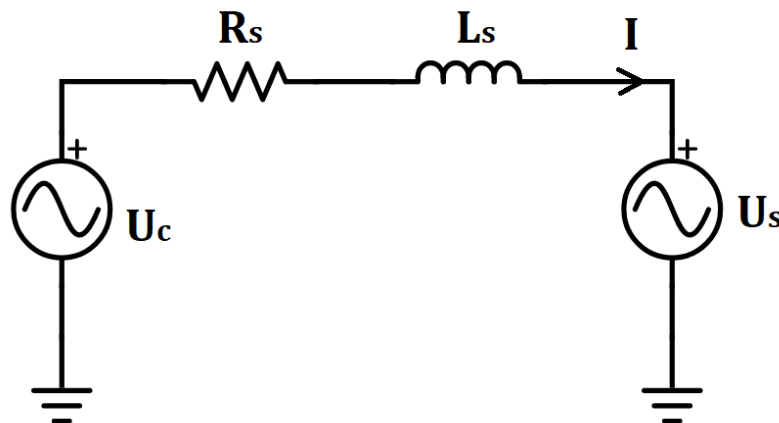


Figure 11: Infinite grid model

For this part we will assume that there is no impedance between the grid and the connection spot. R_s and L_s stand for the impedance between the connection spot and the VSC. Given that the current control has been designed according to this scheme the behavior of the dynamics should remain within the assumptions taken at the design phase. This means that the simulated dynamics should reflect the designed behavior.

The following image illustrates the Simulink model of the infinite grid:

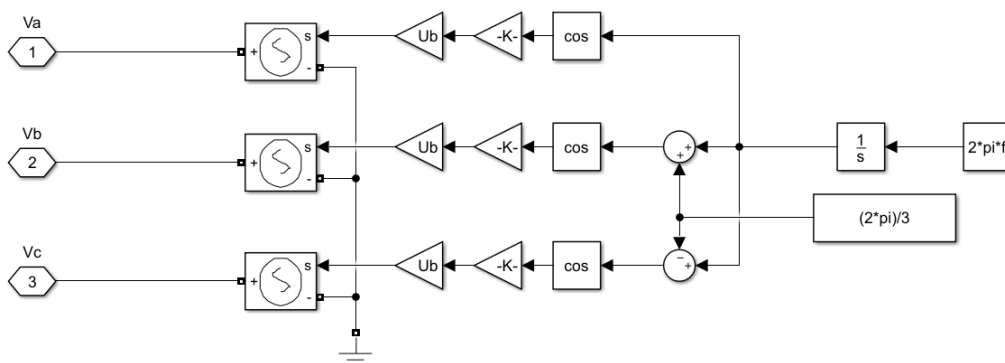


Figure 12: Simulink model of the infinite grid

In this figure we can see that the 3-phase voltage is created through 3 sinusoidal waves with the same amplitude, but phase shifted.

For a better understanding of the VSC functioning the following image is given:

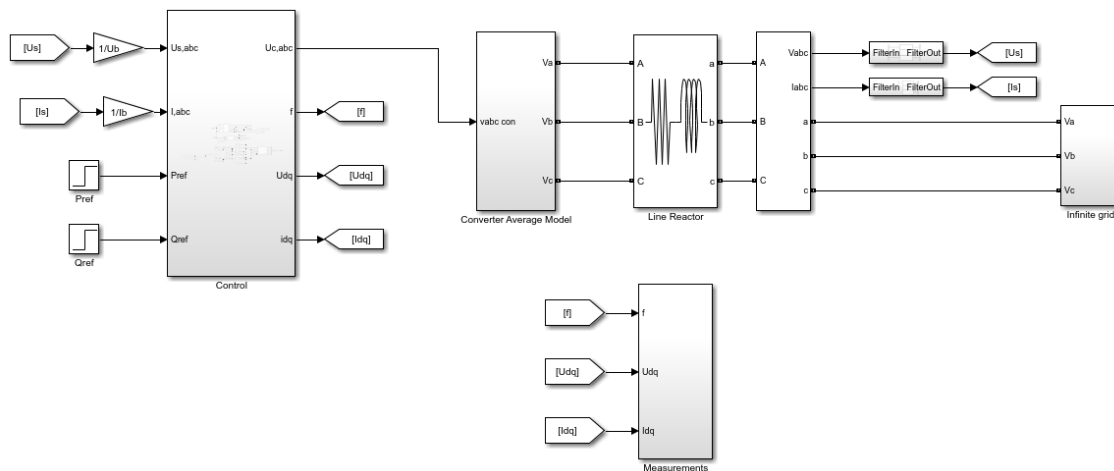


Figure 13: Simulink model overview

In this image the general overview of the simulator is presented. In this figure we can identify all the systems that integrate the simulation. The “Control” block takes both 3-phase voltage and current injected at the connection spot, as well as the references for active and reactive power, and outputs the required VSC voltage, along with some relevant measurements. The “Converter average model” block takes care of transforming the Simulink voltage signal into a 3-phase voltage that can be introduced in any SymPowerSystems block. Finally, the “Measurements” block is used to process all the data from the most relevant variables in the system in order to output graphical information and save the data into other MATLAB compatible formats for further analysis.

In order to evaluate the control system performance, we will proceed to simulate 2 scenarios. The system will part from a state of no power injection. The first scenario will consist in an increase in the value of the active power reference to 20 MW. Sometime after the reference step another increase in the value of reactive power reference will be performed, this time 10 Mvar. The following plots represent the evolution of both P_s (active injected power) and Q_s (reactive injected power) for both events:

First event (step in P_s):

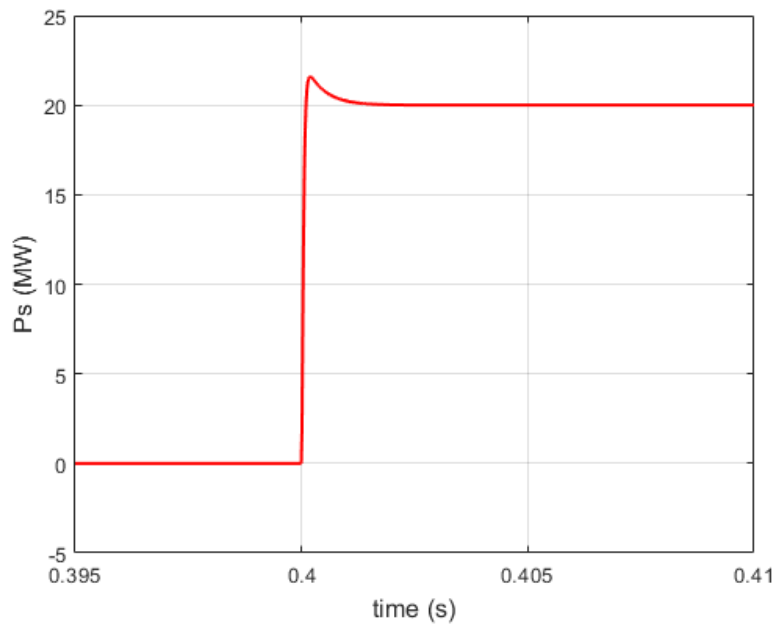


Figure 14: P_s . Step in P_s ref (infinite grid)

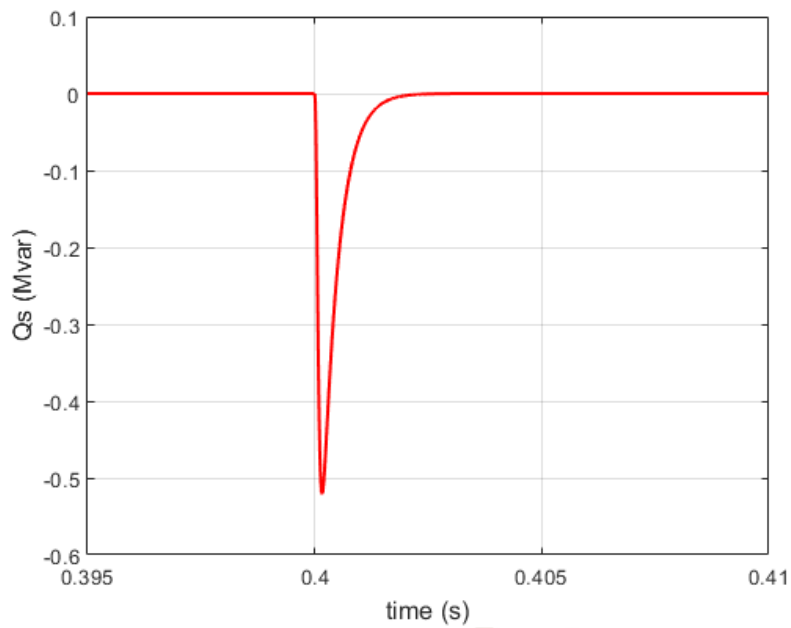


Figure 15: Q_s . Step in P_s (infinite grid)

Second event (step in Q_s):

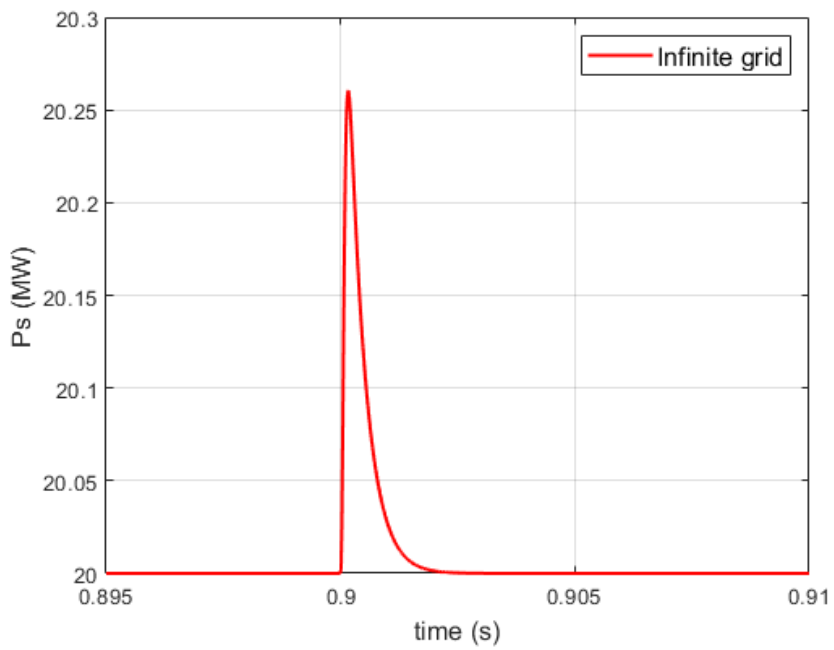


Figure 16: P_s . Step in Q_s (infinite grid)

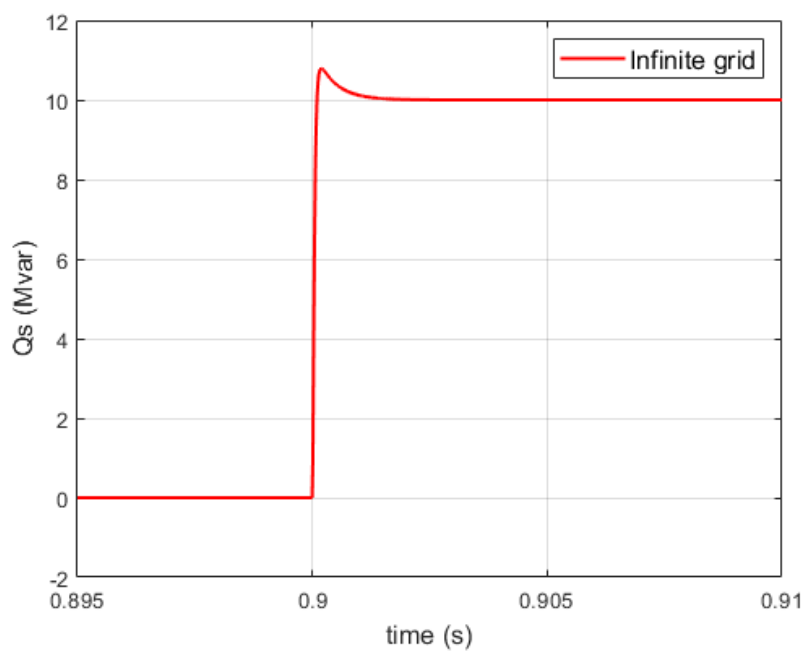


Figure 17: Q_s . Step in Q_s (infinite grid)

We can extract several conclusions from the above graphs:



- Due to the coupling effect (crossed terms in the inner loop) P_s is affected when there is a variation in Q_s ref, and so is Q_s when there is a variation in P_s ref. This coupling is, nevertheless, not very significant.
- The dynamics for both controls are the same, as we expected, since the plant ($P(s)$) is the same in both cases and so are control parameters.



4. Low inertia power systems connected to VSC

In this chapter we will focus on describing the low inertia power system used for the simulations that will further be presented. In order to so, we first have to understand the critical role of inertia in an AC electrical power system. Some real-world examples will be provided, along with the full description of our specific case of study.

4.1 Mathematical modeling

In this section of chapter 4 a brief mathematical explanation of the model will be given. First, some concepts regarding inertia will be presented, and then we will take into consideration the stability of the power system, and the importance of inertia within this stability.

4.1.1 Inertia

Inertia stands for the physical property of objects that tend to maintain a certain state over time. The most accurate definition would then be the property of objects that offers resistance to changing their speed, either if it is the angular or linear speed. In a power systems regulation context inertia stands for the property of any AC power system that resist to change its frequency. This inertia is directly related to the mechanical inertia of the rotating synchronous machines that provide power to the system.

The equation that rules the mechanical behavior of any rotating element is the following:

$$J \frac{d\omega}{dt} = \sum M_i \quad (\text{Ec. 23})$$

This equation implies that the variation of the angular speed of any element times the inertia of the element (J) is equal to the sum of applied torques. In the particular case of a synchronous machine the equation can be stated as:

$$J \frac{df}{dt} = M_m - M_r \quad (\text{Ec. 24})$$

Where M_m is the torque provided by the steam turbine, hydro turbine or other element and M_r is the resistance torque. Note that ω was substituted by frequency, since synchronous machines rotate at speed equal to the power system frequency. If we use per unit variables the torque magnitude can be expressed in terms of power, leaving the following equation:

$$2H \frac{df}{dt} = P_g - P_d \quad (\text{Ec. 25})$$

P_g stands for generated electrical power and P_d for electrical power demand. This equation models the behavior of frequency when differences between generation and demand occur. Note that J has been changed to H , which stands for the electrical inertia of the synchronous machine. If H is expressed in the above terms (per unit variables) its units are seconds (s). There is an equivalent translation between the value of H in seconds and the dynamics of change of frequency whenever an imbalance between generation and demand occurs. The following table offers typical values for H , for different types of turbines:

Generator type	H(s)
Steam turbine	4/10
Gas turbine	2.5/6
Hydro turbine	2/4
Diesel motor	1/2

Table 1: Typical values of H for different machines:

In an electrical power system with more than one synchronous machine we can demonstrate that the total value of the system inertia is equivalent to the algebraic sum of the individual inertia of every generator.

$$H_{TOTAL} = \sum H_i \quad (\text{Ec. 26})$$

For every i generator in the grid.

The particular case of wind generation must be mentioned, because of the possible confusion that wind turbines might induce. While it is true that wind turbines have some inertia, because of the physical properties of the rotor, this inertia is not “seen” by the grid that the generator is connected to. This is due to the fact that AC power generated by the rotating machine present in the turbine is transformed into DC power, which is connected to a DC bus. From this point (the DC bus) the VSC creates the required AC voltage for the grid, according to control specifications.

4.1.2 Stability

After defining some important concepts regarding inertia, we will deepen into the power system stability and its relationship with inertia. Taking into account Ec.25 we can express the relation between frequency dynamics and generated and demanded power by a block diagram:

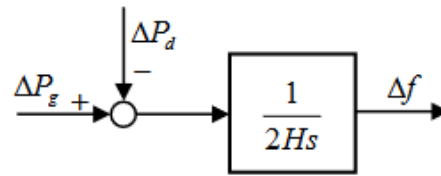


Figure 18: Frequency dynamics block diagram

In this diagram, whose variables are incremental, one can clearly see that any imbalance in generation and demand will integrate into an ever-growing error in the value of grid frequency. In order to control this unstable dynamics, the primary and secondary controls change the generated power in order to stabilize the value of frequency around its nominal value, ensuring correct power system functioning.

The difference between primary and secondary controls rely on their response time, being the secondary one the slowest with time constants of minutes, when the primary one acts in seconds. Because of the dynamics of frequency (order of seconds as we will see later in this document) we will only focus on primary control in order to see the relation between inertia and grid stability. Also, to be more accurate in the process of modeling primary control we must take into account the variation of the load along with the value of the frequency itself, which we call D. The typical value of D implies that the total load decreases along with the value of frequency. If we take all these terms into account, the block diagram of the dynamics of the frequency will remain as follows:

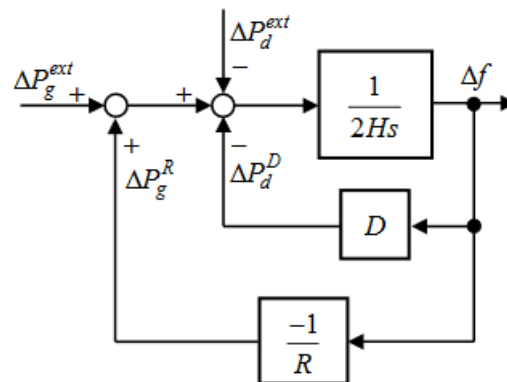


Figure 19: Complete block diagram

Being R (droop) the term related to the primary control, which is a proportional control system. We can see that the closed loop system will present the following transfer function:

$$F(s) = \frac{K}{1 + 2KHs} \quad (Ec. 27)$$



Where the input is the power imbalance and the output is the variation in frequency. The term K stands for the following expression:

$$K = \frac{1}{D + \frac{1}{R}}$$

From this transfer function we can see that the value of the time constant, which defines the dynamics of the frequency is proportional to the inertia term (H). Also, we can see that as long as the value of K is positive, which it is, the system is stable. Nevertheless, the complete block diagram would have to include the transfer functions that stand for the dynamics of the primary control of the generators. If the value of inertia is too low, the closed loop system might become unstable. Further in this document some simulations will be performed in order to conclude whether if inertia is relevant to the system stability or not.



4.2 Low inertia power systems

In this chapter some examples of low inertia power systems will be provided, along with their evolution over time and their relationship with the development of renewable energies.

One of the best examples of a low inertia power system is the UK electric grid. Because of its isolated characteristics the UK has faced problems regarding low inertia for many years, and those will probably increase in the next few. Along with the fact that there is only a little interconnection with continental Europe, Great Britain has also increased their share of renewable energies into power generation in the last years. The following graph shows the evolution of this share in the last decade:

Chart 6.1 Renewables' share of electricity generation

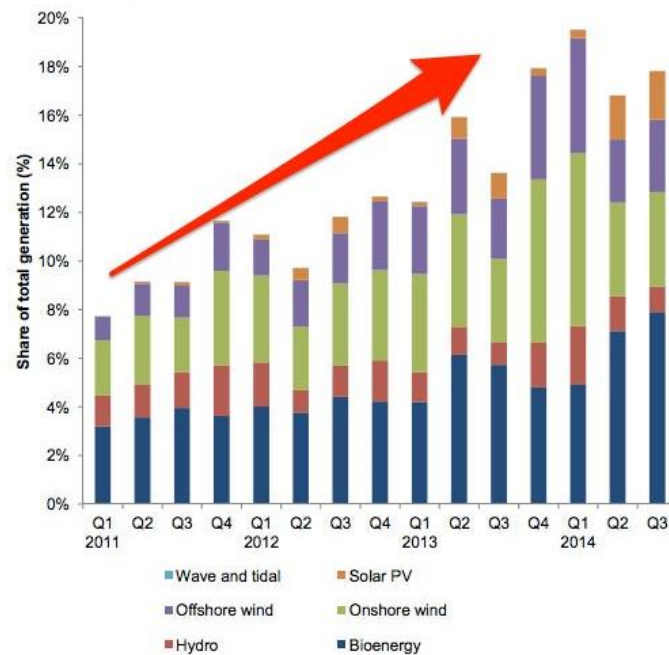


Figure 20: Share of renewables in the UK [12]

In this graph it is notable how the amount of renewable generation has increased in the first half of the decade. Also, the contribution of wind energy should be remarked, specially the increasing offshore wind energy production. After presenting the evolution of renewables in the UK, we can deepen into inertia matters for this case. The following figure shows different dynamics in the response to critical events in different locations in the island of Great Britain:

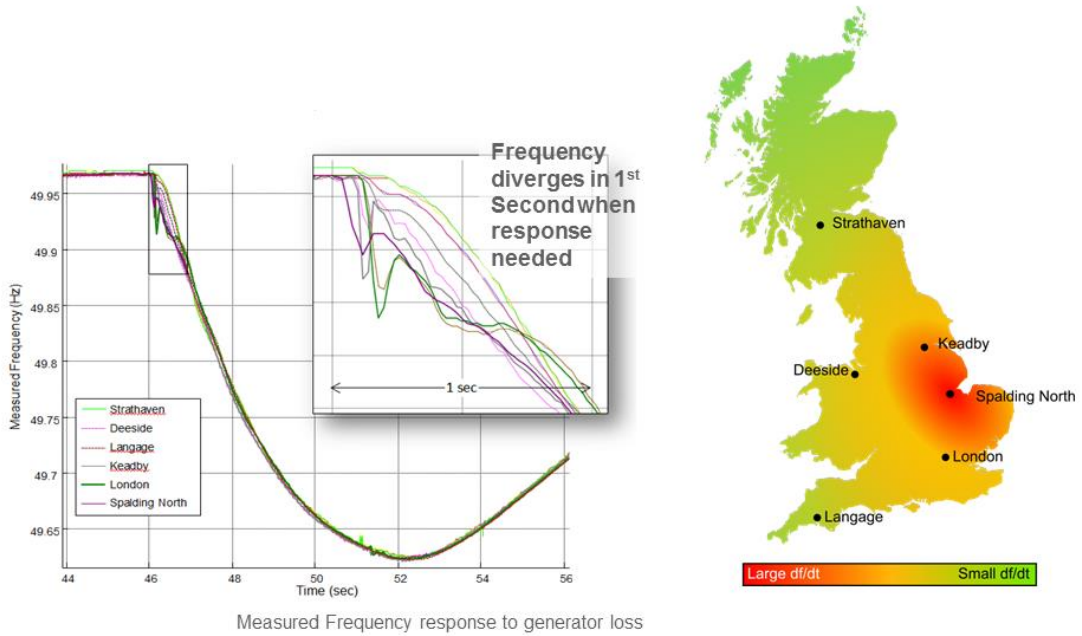


Figure 21: Dynamic differences regarding inertia in the UK [13]

In this figure we can see that there are critical differences in the dynamics of various locations. This is due to the amount of inertia that generators in those areas present. In the “heat map” colors approaching red are the areas with a higher RoCoF (Rate of Change of Frequency), while the ones that are greener have a lower RoCoF. The following image will provide some more information about the distribution of wind energy in the UK:

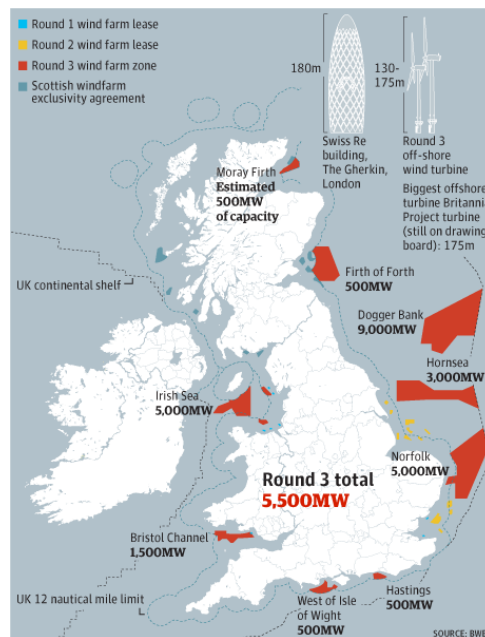


Figure 22: Distribution of offshore wind generation in the UK [14]

Taking both figures into account we can see there is a clear relationship between wind generation and the dynamics of the response to critical events. It is notable that the areas that present higher values for RoCoF are the ones closest to some of the most relevant offshore wind generation farms in the northern sea. This is a very intuitive way of seeing the relation between grid inertia and the share of renewables: the higher the share of renewable energies, the lower the total amount of inertia in the grid.

The case of the UK, however, is not unique, as there are many other power systems facing problems regarding inertia. The Nordic grid, for example has increased its share of renewables in the last decades, as shown in the following figure:

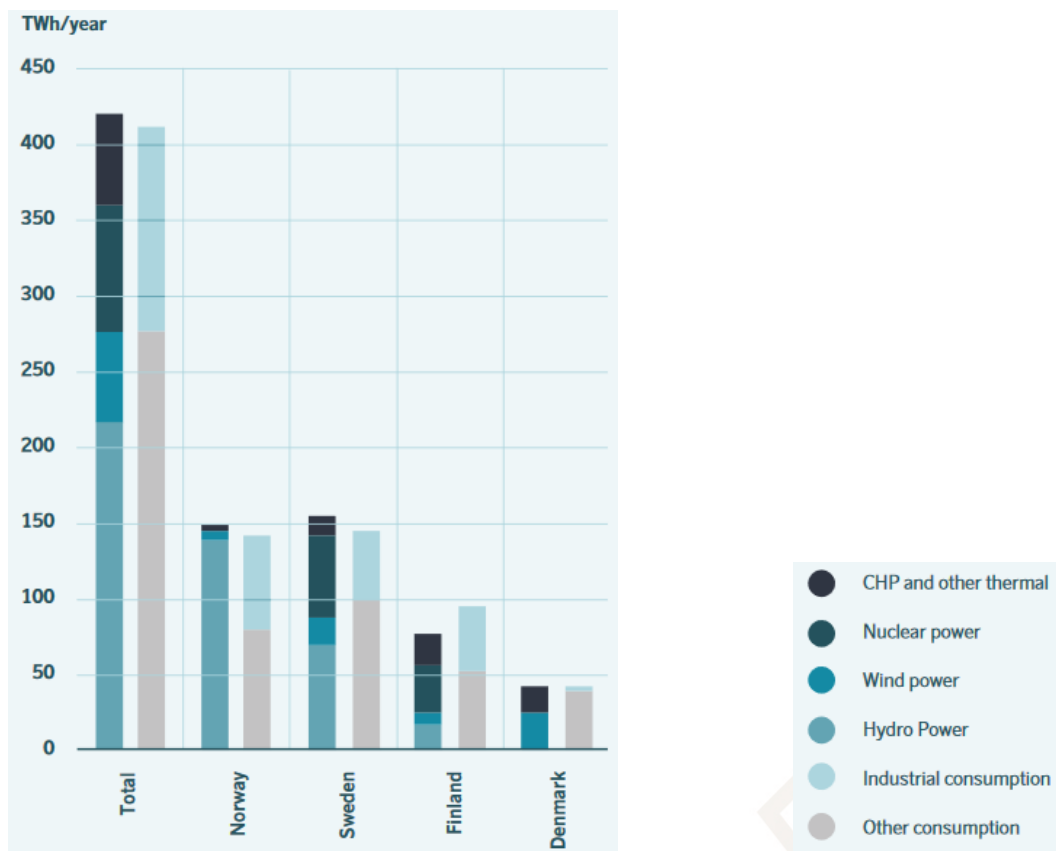


Figure 23: Share of renewables in the nordic grid [15]

In this graph the total generated and consumed power in the Nordic grid predicted for year 2025 is shown. It is noticeable that the share of wind generation is very significant, leading to low inertia issues [16]. Some estimations point that in year 2025 the grid will be operating under the minimum required volume of kinetic energy (predictions round 120-145 GWs) for up to 19% of the operating time, while in 2009 this number peaked at 12%.

In the case of the Nordic grid some solutions are currently being considered. Some propose establishing minimum requirements for kinetic energy in the system, and



others offer the possibility of limiting the power output of the largest units (imported energy through HVDC and generators) during low inertia situations.

In the UK similar ideas are being considered by system operators. Recently, National Grid has offered contracts to different companies in the UK, for those companies to provide inertia without the need to simultaneously providing electricity [17]. National Grid claims to be the first system operator to perform such contracts.



4.3 Case of study

For the proposed scope of this dissertation several simulations have to be performed. To finish this chapter, we will proceed with a brief description of the specific electric power system that the simulations will be performed on.

The case study power system is based on the Kundur power system, provided by the Simulink SymPowerSystems tool.

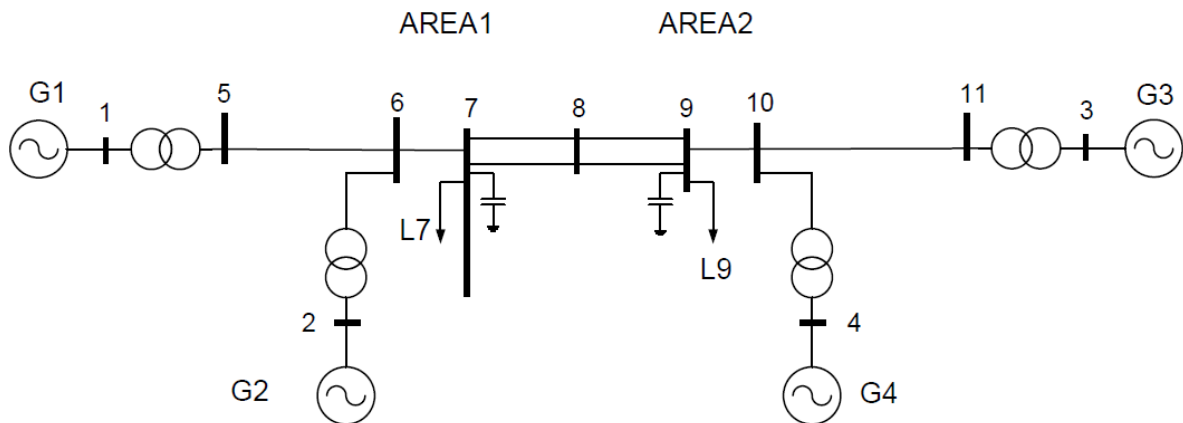


Figure 24: Kundur power system

In this example there are 2 separate areas, each one of them with their own generators and loads. For our purpose one of the areas has been substituted by a VSC. The remaining power system looks like the following:

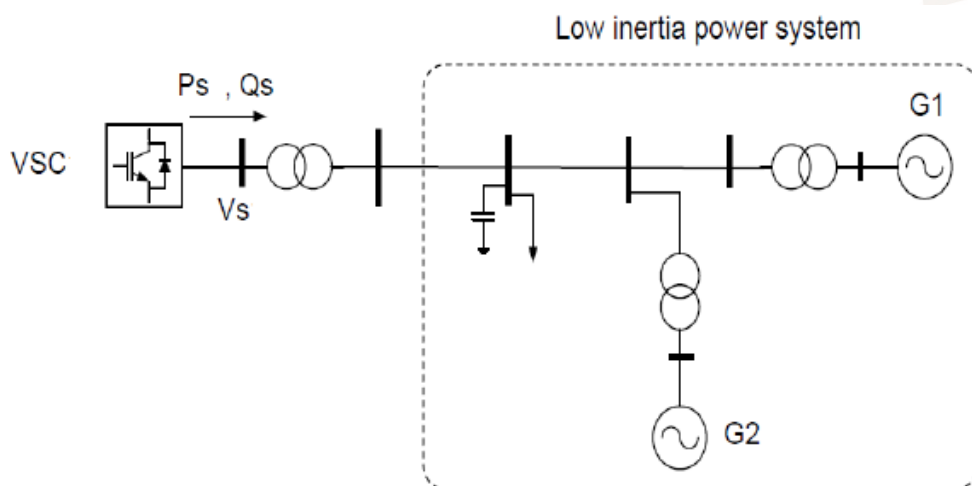


Figure 25: Low inertia case study power system

As we can see there are 2 synchronous generators, connected by transformers, just like the VSC. There are 2 loads: a reactive power load and an active power load, which will model the demand. In order to perform simulations over this system a Simulink model must be created. To do so, the SymPowerSystems tool has been used. This tool allows us to emulate the behavior of electrical elements, such as transformers, generators, lines and loads with high precision. The following scheme represents the proposed Simulink model for the system:

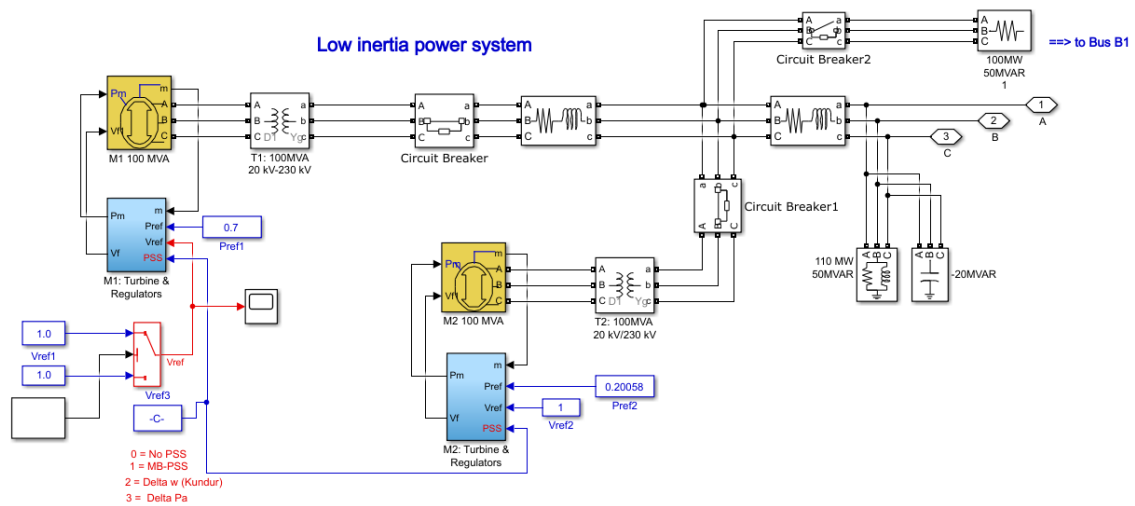


Figure 26: Simulink model of the low inertia power system

As we can see, the electrical model has been translated into Simulink blocks. Note that some of the “wires” that connect blocks carry information (signals) and others are the electrical equivalent to a physical wire. In the image we can see that there are 2 synchronous generators. Each one of them has a corresponding turbine and regulators block, which model the behavior of the steam turbine that powers the generator. All the lines have been modeled through a lumped PI model. Also, there are several loads, which will model the demanded power. The ABC connectors will allow us to connect the VSC to this low inertia power system. The values of the different parameters that characterize the system can be found in the annex.

5. Simulation of Voltage Source Converters connected to Low inertia power systems

In this chapter we will perform several simulations over the already presented low inertia power system. The main goal is to obtain results that will allow us to extract conclusions regarding the role of inertia in the overall power system performance and the VSC control. Just like in chapter 3 changes in the demand/generation will be performed to check the system response in several scenarios.

5.1 Scenario 1: Changing the value of H

In this part the value of H for every generator will be changed, from its original value to lower ones. The goal is to perform a sensitivity analysis on the importance of the specific value of the system inertia. The original value of the inertia constant (H) for both synchronous machines are set to 6.5 s. Note that this value is within the range of values for H, provided in table 1.

Analogously to chapter 3, two step functions will be applied to the reference value of active and reactive power injection. Also, we will implement a voltage control (substituting reactive power injection control), in order to test their differences in performance and limitations for both. The reason to test a voltage control as well as a reactive power control relies on the fact that the grid is not infinite, therefore the voltage at the connection point does not have to be the nominal one. In this context it could make sense for the system operator to be interested in controlling the voltage in one specific node of the grid.

For this scenario the VSC will part from the following conditions:

$$P_{s0} = 20 \text{ MW} \quad Q_{s0} = 0 \text{ Mvar} \quad U_{s0} = 1 \text{ pu}$$

After the steady state has been reached a first increase in the reactive power reference of 10 Mvar is performed, at $t=0.4$ s. After the steady state is reached again a decrease in the active power reference of 10 MW is performed, at $t=0.7$ s. The below results correspond to the most significant variables for each one of the presented cases (different values of H):

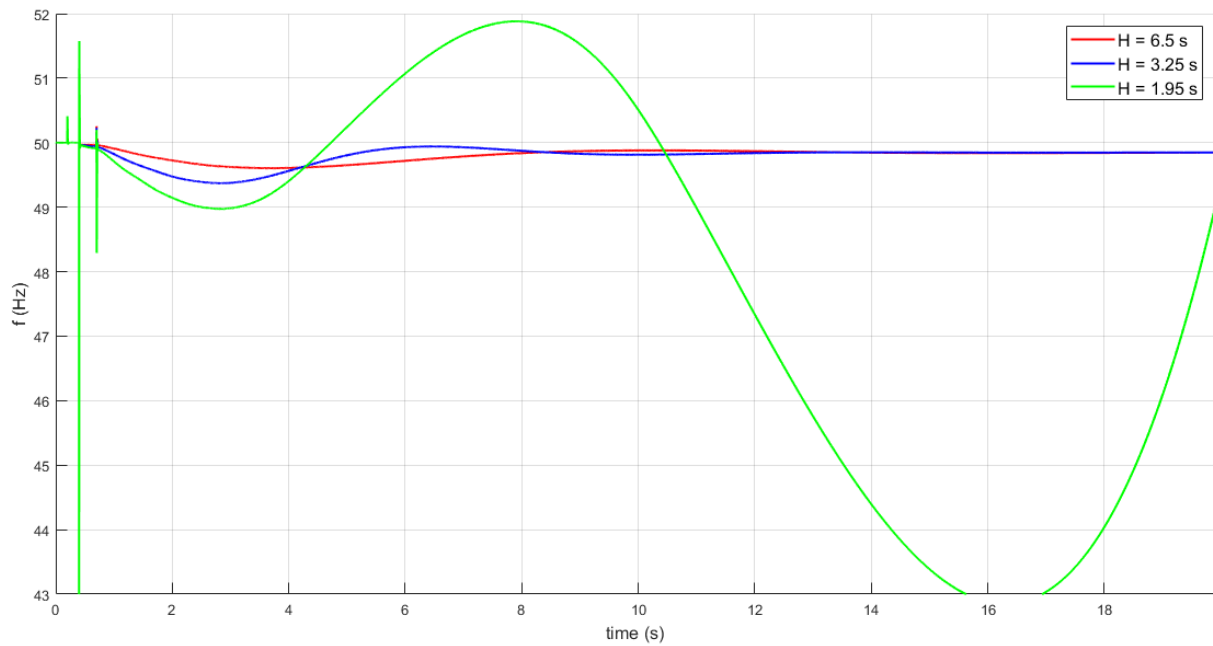


Figure 27: Frequency plot for scenario 1

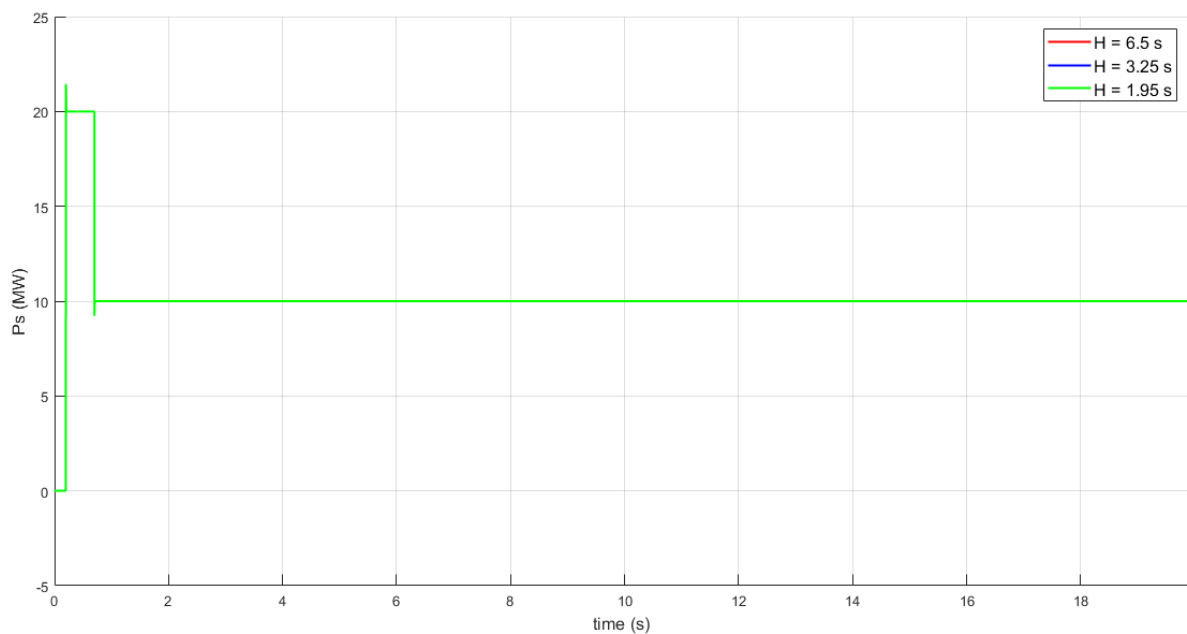


Figure 28: Active power plot for scenario 1

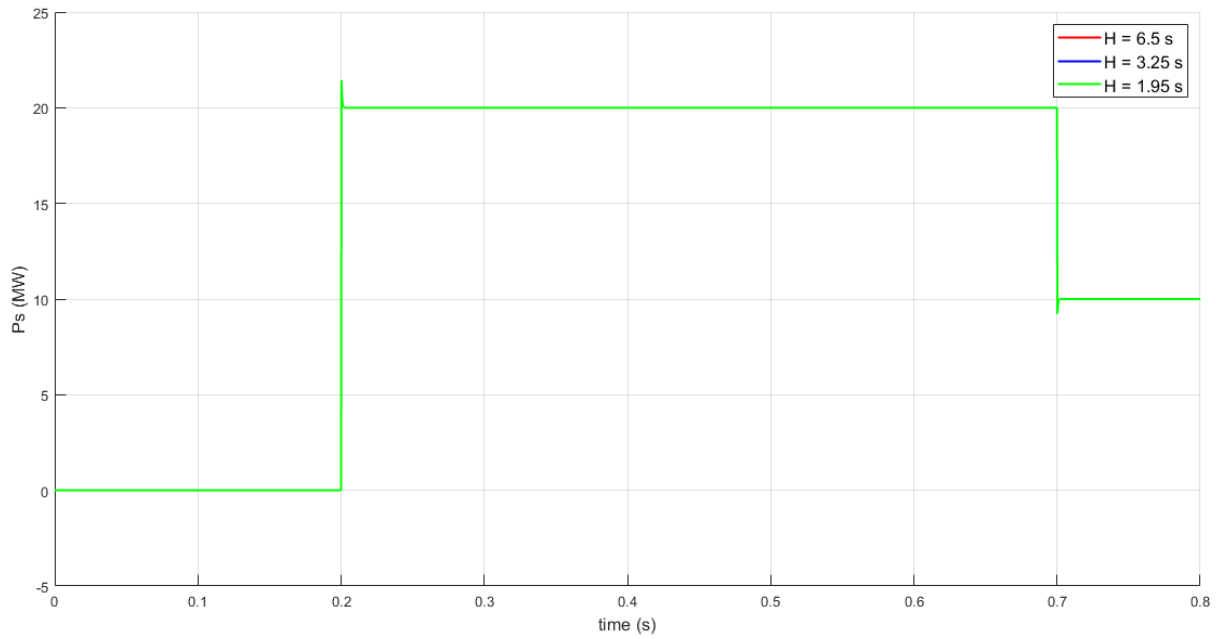


Figure 29: Active power plot for scenario 1, detailed

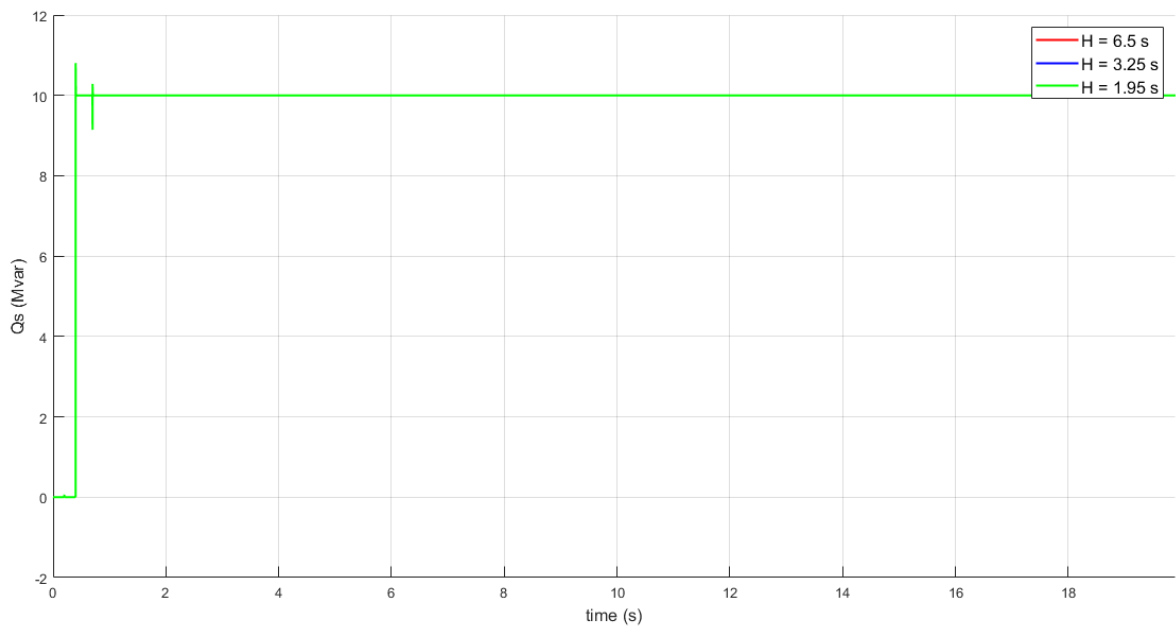


Figure 30: Reactive power plot for scenario 1

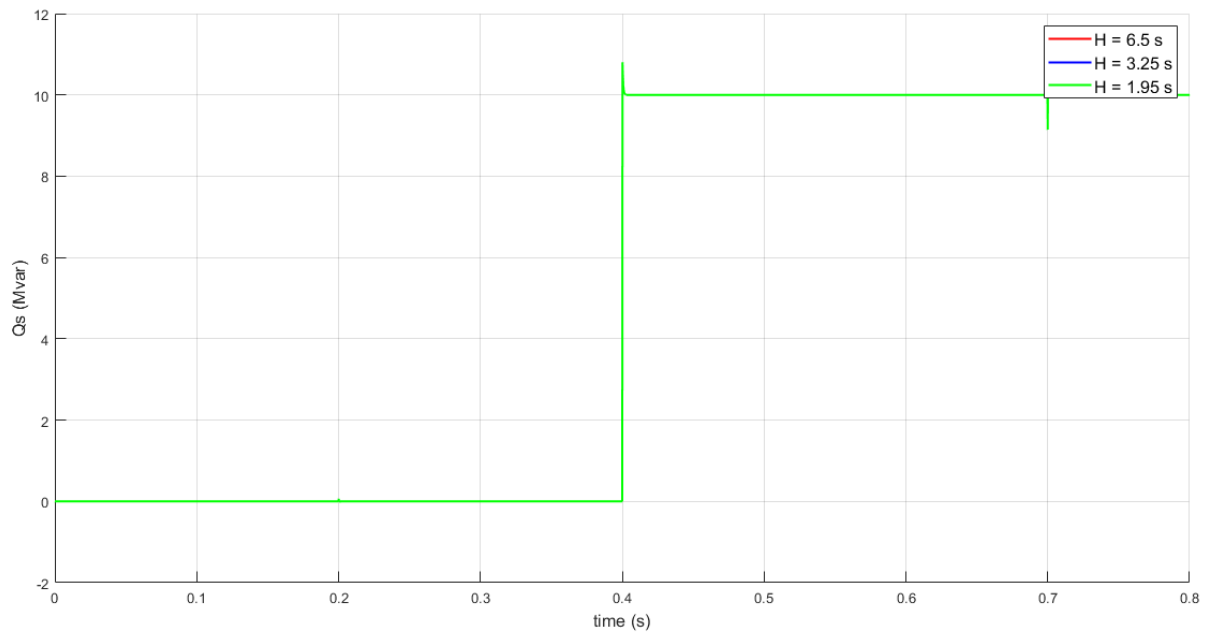


Figure 31: Reactive power plot for scenario 1, detailed

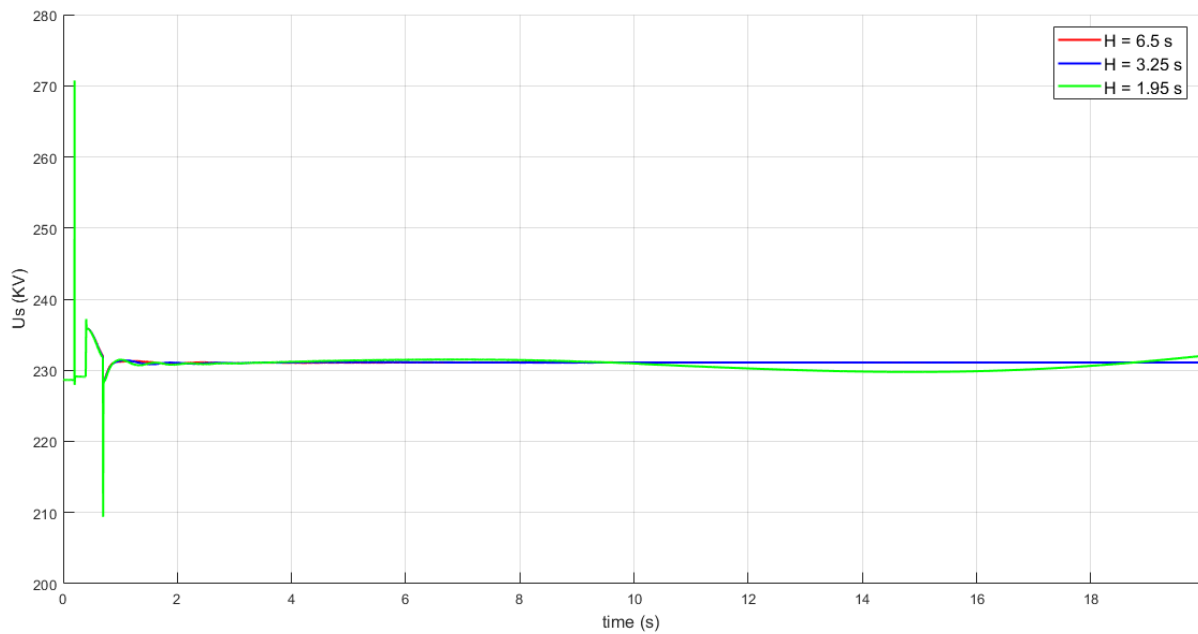


Figure 32: Voltage plot for scenario 1



Note that for both P_s and Q_s the time axis has been reduced to less than a second. This is due to the fact that after this time horizon the value of both variable doesn't change, therefore is not very interesting to see the remaining data. From those graphics we can extract the following conclusions:

- The control dynamics and operation are not affected by the total amount of inertia in the grid, as the graphics from different cases are almost overlapping each other.
- The total inertia in the grid is critical for frequency stability. At some point between 30% and 50% of initial inertia values this stability is lost in this particular case of study.
- Note that there is no error in steady state for both active and reactive power. This result is expected, since there is an integral part in the control system for both variables, which ensures this property.



5.2 Scenario 2: Changing the nominal power

For this part, the value of H will be fixed for all the generators at a value of 30% of their initial value (6.5 s each). In this simulation scenario the nominal power of every generator will be changed to both half and twice as much as the original case. The expected variation of inertia should follow this equation:

$$H_{system}(pu) = H_{nominal}(pu) \frac{S_{ng}}{S_B} \quad (Ec. 28)$$

Where S_{ng} stands for nominal power of the generators, S_B for the Base power (100 MVA) and $H_{nominal}$ for the nominal inertia of the generators.

The dynamics of the events that will be simulated, this is, the steps made in order to test the control, are the same as in chapter 5.1. Analogously to chapter 5.1 the results of the simulations will be given as a series of graphical information about the most important variables. Those results are the following:

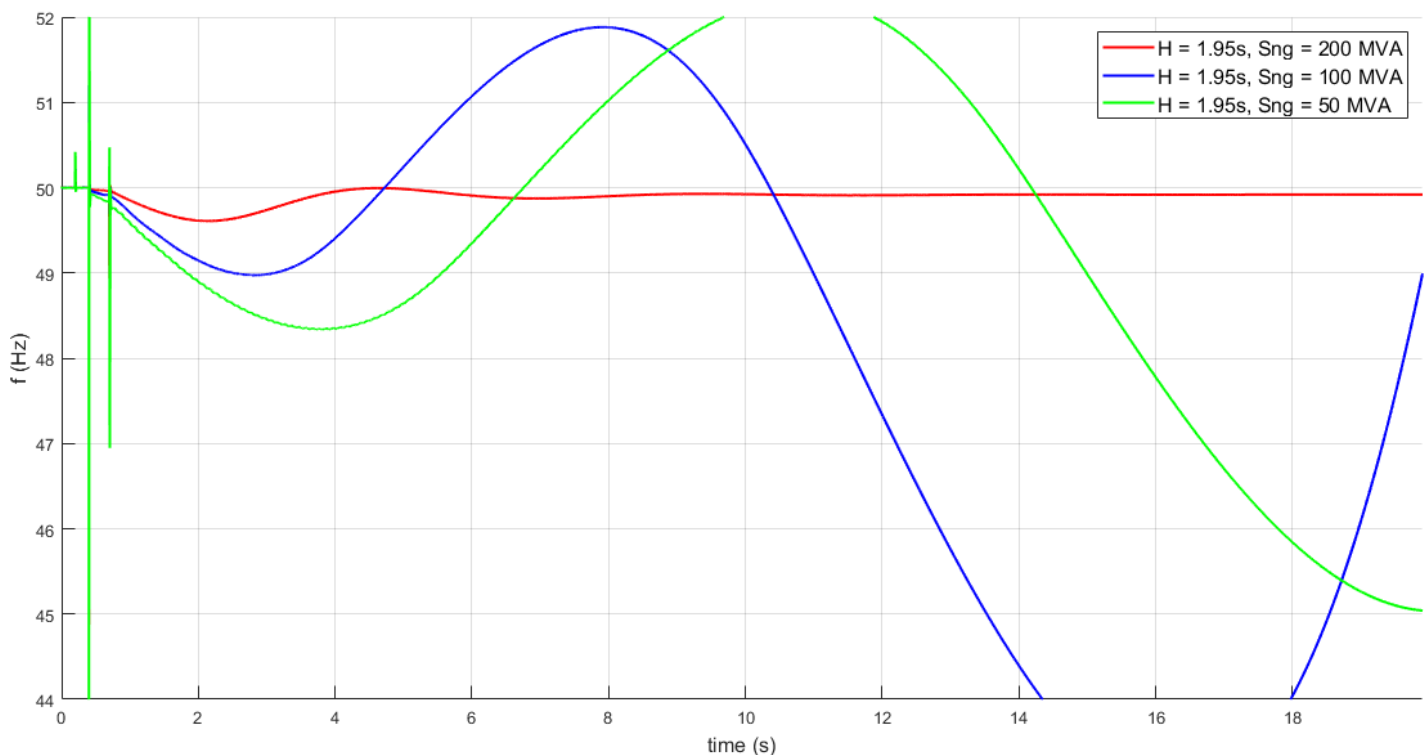


Figure 33: Frequency plot for scenario 2

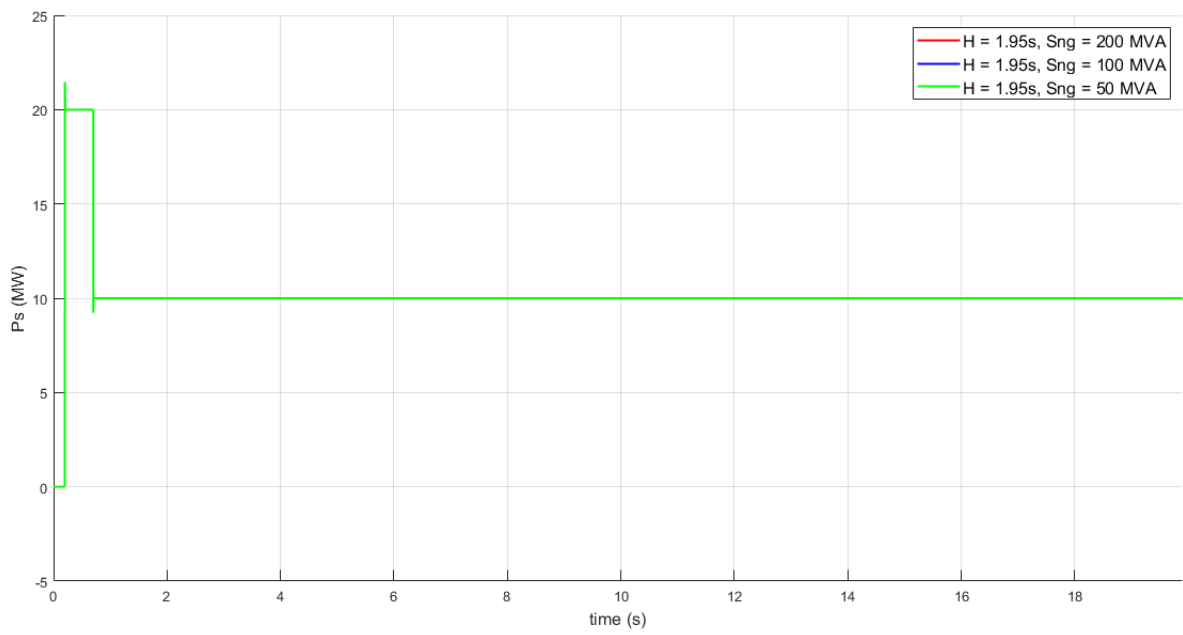


Figure 34: Active power plot for scenario 2

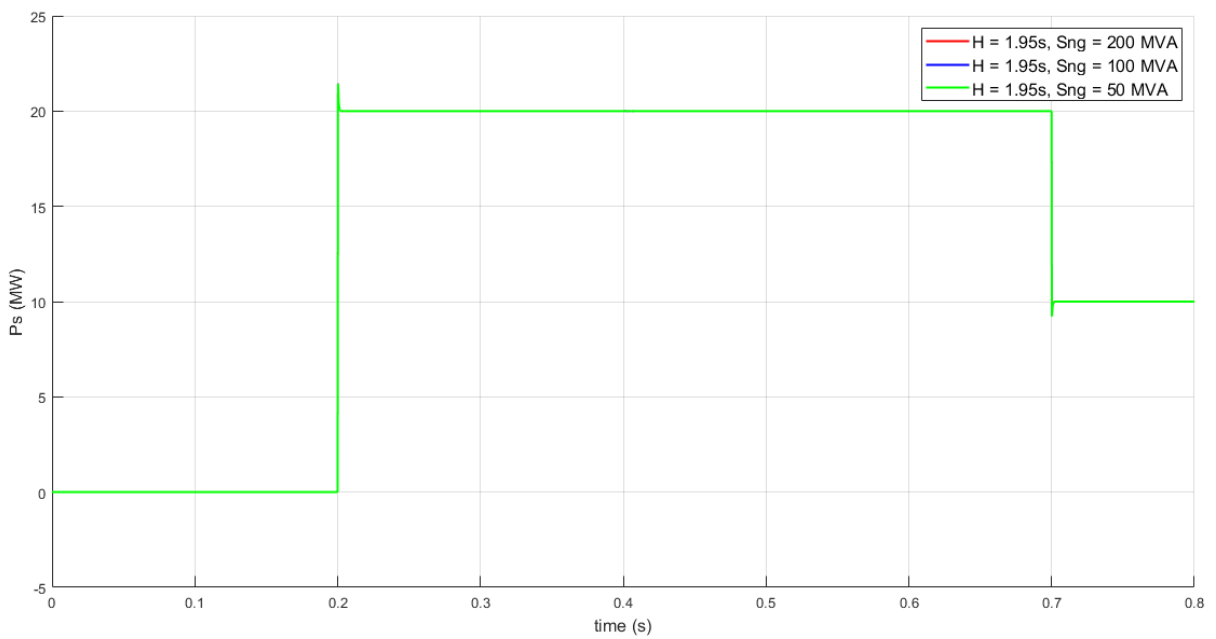


Figure 35: Active power plot, scenario 2, detailed

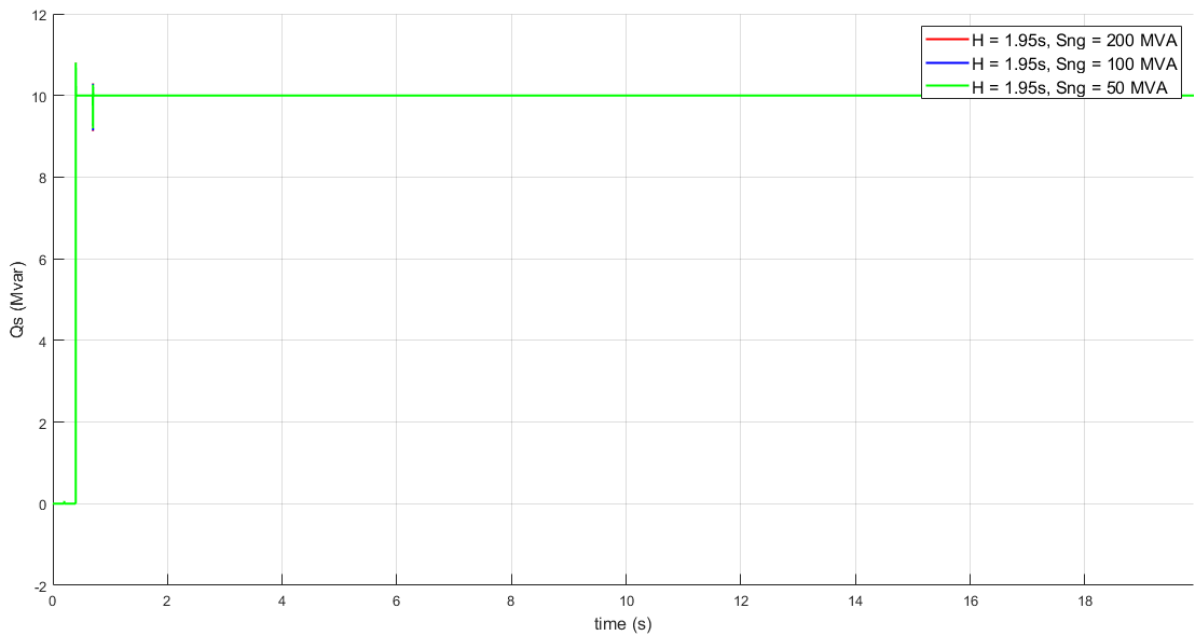


Figure 36: Reactive power plot for scenario 2

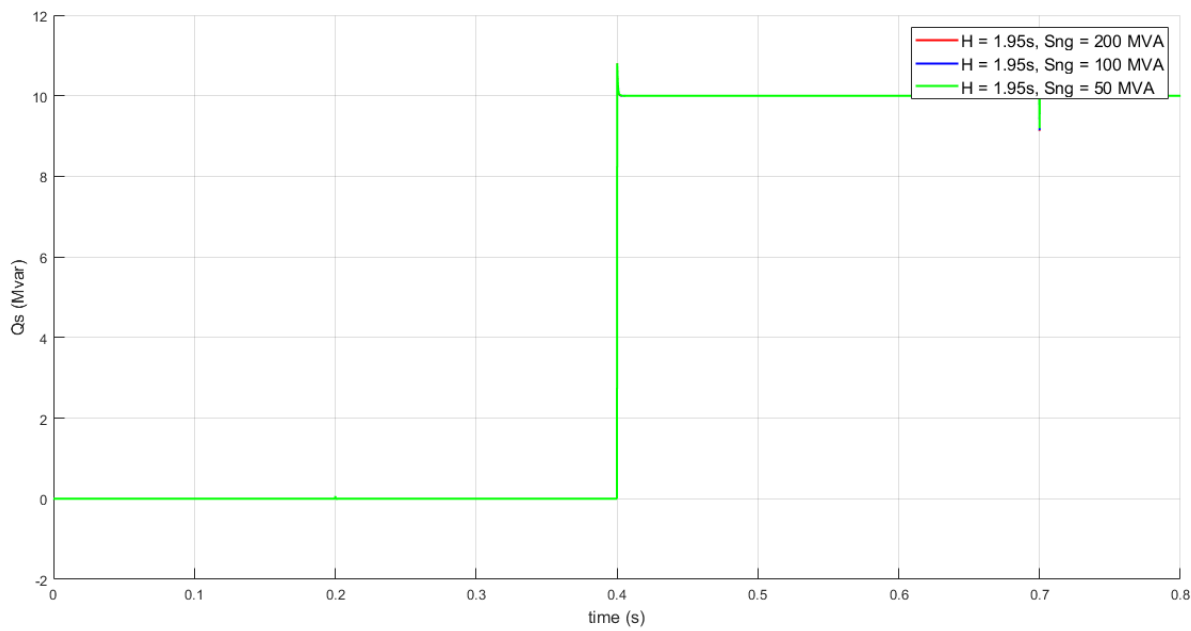


Figure 37: Reactive power plot, scenario 2, detailed

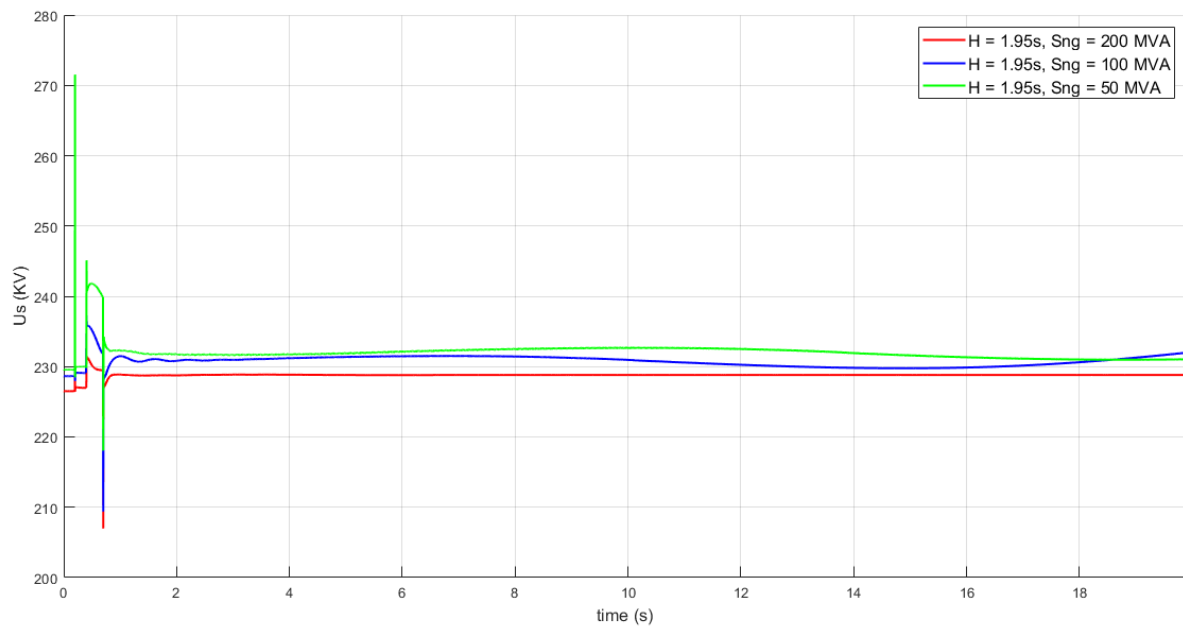


Figure 38: Voltage plot for scenario 2

Regarding these results we can extract the following conclusions:

- We can see that changing the nominal power of the generators can change the “weight” of those generators in the overall system stability. For the case where the weight of the generators is increased the overall inertia also increases and the system becomes much more stable and robust (from the frequency point of view).
- Analogously to the results obtained in the last chapter we can see that this difference in the total value of inertia does not affect the dynamics of the VSC control.
- Also regarding the VSC control for active and reactive power, there is no error in steady state for both variables, just as expected.



5.3 Conclusions

The following conclusions have been obtained from the results of this chapter:

- As the inertia of the system decreases, the stability of the system is jeopardized. This is due to the fact that any perturbation will produce undamped oscillations in the frequency.
- This instability is mainly linked to the low-inertia power system and not to the control of the VSC. In fact, the VSC is able to control active- and reactive-power injections successfully



6. Conclusions and future work

Conclusions

This project analysed the dynamic behaviour of a current controlled voltage source converter (VSC) connected to a low-inertia power system. The VSC considered has a rating comparable to the total rating of the synchronous machines that compose the low-inertia power system. The analysis has been carried out in MATLAB + Simulink + SimPowerSystems, using detailed electromagnetic models of the VSCs. A sensitivity analysis has been carried out analysing the stability analysis of the system by means of non-linear time-domain simulation for different scenarios of reduced total inertia of the power system.

The conclusions obtained in this work are as follows:

- As the total inertia of the power system decreases, the stability of the system is jeopardised
- This is due to the fact that, as the total inertia of the power system is reduced, small disturbances produce significant slow oscillations
- The instability is produced in the power system
- However, the stability of the VSC connected to the grid is not jeopardised as the total inertia of the power system is reduced. In other words, even for low inertia of the power systems, the controllers of the VSC behave properly

Future work

The results obtained in this Project opens room for further research. Mainly, a more detailed analysis of the stability of low-inertia power systems with VSCs should be carried out.

Specific proposals for further research are as follows:

- Small-signal stability analysis: Small-signal stability analysis techniques should be carried out in order to fully understand the dynamics involved in the stability of this type of systems.
- Large-signal stability analysis: A thorough study on the stability of this type of systems against large disturbances (such as generator tripping or short circuits) should be carried out.
- Detailed analysis of different types of stability phenomena in this type of systems:
 - Stability of the VSC connected to the low-inertia power system
 - Angle stability of this type of systems (small and large disturbances)
 - Frequency stability
 - Voltage stability



- Detailed analysis of the impact of phase-locked loop (PLL) of the VSCs connected to low-inertia power systems
- This work analysed the behaviour of current controlled VSCs (also known as “grid following”) connected to a low-inertia power systems. Future studies should analyse the behaviour of low-inertia power systems containing both, “grid following” VSCs and voltage-controlled VSCs (also known as “grid forming”)



7. Annex

7.1 System parameters

In this chapter the parameters of the case of study low inertia power system will be provided. The elements that integrate the power system are the following:

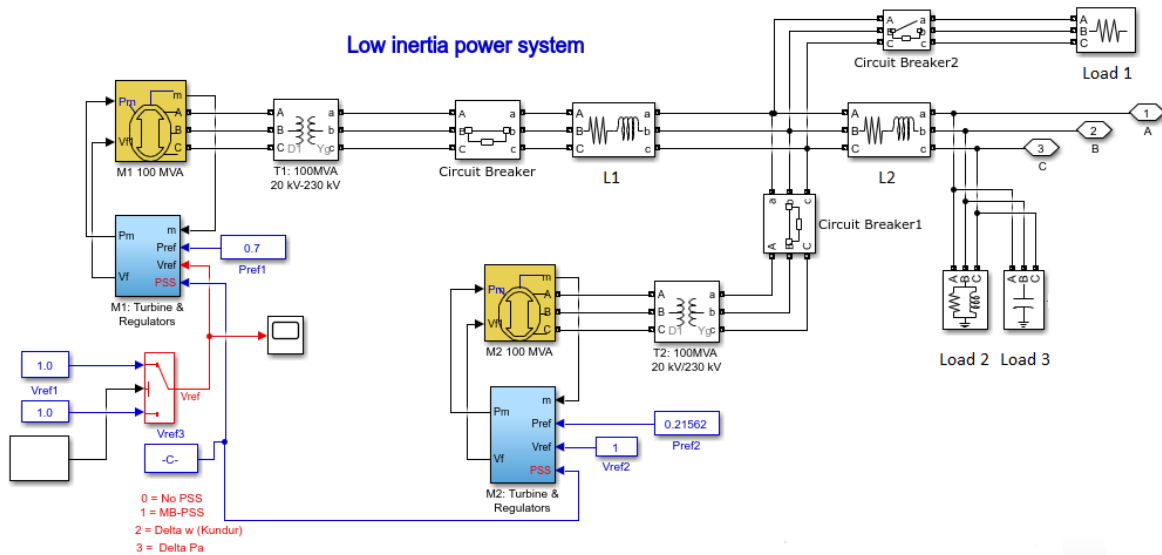


Figure 39: Low inertia power system elements

And the corresponding parameters are the following ones:

Generator M1	
Parameter	Value
Nominal power (MVA)	100
Nominal voltage (KVrms)	20
Nominal frequency (Hz)	50
X_d (pu)	1,8
X_d' (pu)	0,3
X_d'' (pu)	0,25
X_q (pu)	1,7
X_q' (pu)	0,55
X_q'' (pu)	0,25
X_I (pu)	0,2
Friction factor (pu)	0
Pairs of poles	4
Inertia coefficient (initial value) (s)	6,5

Table 2: Parameters for generator M1

Generator M2	
Parameter	Value
Nominal power (MVA)	100
Nominal voltage (KVrms)	20
Nominal frequency (Hz)	50
Xd (pu)	1,8
Xd' (pu)	0,3
Xd'' (pu)	0,25
Xq (pu)	1,7
Xq' (pu)	0,55
Xq'' (pu)	0,25
XI (pu)	0,2
Friction factor (pu)	0
Pairs of poles	4
Inertia coefficient (initial value) (s)	6,5

Table 3: Parameters for generator M2

Transformer T1	
Parameter	Value
Nominal power (MVA)	100
Nominal frequency (Hz)	50
Nominal V1 (KVrms)	20
R1 (pu)	10^{-6}
L1 (pu)	0
Nominal V2 (KVrms)	230
R2 (pu)	10^{-6}
L2 (pu)	0,15
Rm (pu)	500
Lm (pu)	500

Table 4: Parameters for transformer T1

Transformer T2	
Parameter	Value
Nominal power (MVA)	100
Nominal frequency (Hz)	50
Nominal V1 (KVrms)	20
R1 (pu)	10^{-6}
L1 (pu)	0
Nominal V2 (KVrms)	230
R2 (pu)	10^{-6}
L2 (pu)	0,15
Rm (pu)	500
Lm (pu)	500

Table 5: Parameters for transformer T2

Lines are modeled as simple RL branches with the following parameters:

	R (Ohms)	L (H)
Line L1	1,322	0,035
Line L2	0,014	0,014
VSC-Grid	5,290	0,033

Table 6: Parameters for all lines



The parameters for the VSC are the following:

VSC	
Parameter	Value
Nominal power (MVA)	100
Nominal voltage (KV)	230
Filter resistance (Ohms)	5,290
Filter inductance (H)	0,336
Ki (integral controller gain)	$3,141 \cdot 10^4$
K (proportional controller gain)	13,95

Table 7: VSC parameters



7.2 Budget

In this chapter the cost of making this project is explained with detail. The total cost of the resources needed to perform this dissertation are the following:

$$C_{TOTAL} = C_{eng} + C_{mat} \quad (Ec. 29)$$

Where C_{TOTAL} stands for the total cost, C_{eng} for the cost of the engineering process and C_{mat} for the cost of the materials required (mostly software). The following table describes the list of materials required:

	Quantity	Price
MATLAB license	1	2.000 €
Simulink	1	3.000 €
Simscape	1	2.000 €
Simscape electrical	1	3.000 €
TOTAL		10.000 €

Table 8: Cost of the materials

The cost of the hardware components required for performing the simulations and writing this document has not been included, due to the fact that a personal computer was used for this purpose. Assuming a total number of hours spent on the project as an estimate of 260, and a price for hour of work of 13 € (approximated value), we can derive the total cost the following way:

$$C_{TOTAL} = 13 \frac{\text{€}}{h} * 260h + 10.000 \text{ €} = 13.380 \text{ €}$$

7.3 Sustainable Development Goals

In this chapter of the annex we will analyze the alignment of this project with the Sustainable Development Goals, provided by the United Nations. The objective of the SDG is to provide a clear path in which people can orient their work to make a better world for future generations in terms of matters such as poverty, climate change or education. The following figure shows the different SDG proposed:



Figure 40: SDG

For this project, the SDG goals that are related are summarized in the following table:

SDG dimension	SDG identified	Role	Goal
Biosphere	SDG 7.	Primary	Ensuring access to electricity for all the population in the world. Create the required infrastructure for clean energy production
Society	SDG 9.	Secondary	Creating industries innovation and infrastructure. Increase scientific research in order to improve the technological capacity of our society.

Table 9: SDG alignment



In the table we can see that there are 2 main SDG with a certain level of relation with this project. The most relevant one is SDG number 7, which promotes the access to clean and sustainable energy to all the population in the world.

Currently, around 87% of total world population have access to electricity at some degree. The next few years will be characterized by the increase in the production of electric energy in developing countries, and some of that production will be from renewable sources. Along with this increase in developing countries, the rest of the world will keep increasing their renewable generation share into their respective electric power systems. In many cases there will be technological challenges, and problems regarding low inertia will arise. Therefore, the alignment of this dissertation this SDG number 7 is very high. In order to increase the share of renewables in power generation to ensure clean energy, there must be solutions and simulation tools prepared for low inertia scenarios, and this project intends to be a useful tool for either future research or simulation of low inertia power systems.

The other SDG aligned with this project is number 9, which is related to the development of science and technology. Innovation and infrastructure are key drivers of economic growth and development and they should be promoted in order to reach a more efficient society. This SDG is particularly related to number 7, in the sense of reaching more efficiency will lead to a less polluting production of resources. In this project there are several contributions to electrical engineering topics and some interesting ideas and insights which can lead to some degree of technological development in topics regarding engineering, electronics, power systems and control. Nevertheless, the implication in this SDG is less relevant than the one with SDG number 7.





8. Acknowledgments

This MSc dissertation could not be possible without the help of Strathclyde University, specifically towards the figure of its illustrious professor Dr. Agustí Egea Álvarez, which has been critical in the process of reviewing the document and the simulations models, and providing the general path and guidelines for developing the different tasks involved in the project.

Also, the IIT as an institution has provided the tools necessary for the realization of this project, with special gratitude to Javier Renedo, who has supported every phase of the project with his extended knowledge in all the topics involved regarding power systems and whom has also provided important guidelines for the accomplishment of the dissertation.

The supervision work of Javier Renedo was supported by Madrid Regional Government under PROMINT-CM Project Ref. S2018/EMT-4366 and by the Spanish Government under RETOS Project Ref. RTI2018-098865-B-C31.



9. References

- [1] GWEC, "Global Wind Statistics 2019," Global Wind Energy Council (GWEC), Brussels, Belgium, Tech. Rep., 2020
- [2] IEA, "Solar PV drives strong rebound in renewable capacity additions", International Energy Agency (IEA), Masdar City, Abu Dhabi, Tech. Rep., 2020
- [3] F. Milano, F. Dörfler, G. Hug, D. J. Hill and G. Verbič, "Foundations and Challenges of Low-Inertia Power Systems," Proc. IEEE/PES Power Systems Computation Conference (PSCC), Dublin, Ireland, June, 2018, pp. 1-25.
- [4] Agustí Egea-Alvarez, Adrià Junyent-Ferré and Oriol Gomis-Bellmunt, "Active and reactive power control of grid connected distributed generation systems", 2-3.
- [5] Vasudeo B. Virulkar, "Modeling and Control of DSTATCOM with BESS for Mitigation of Flicker" , ResearchGate, 2009
- [6] Chown, Graeme & Wright, Jarrad & van Heerden, Robbie & Coker, Mike. (2018). System inertia and Rate of Change of Frequency (RoCoF) with increasing non-synchronous renewable energy penetration. CIGRE Science and Engineering. 11.
- [7] Adolfo Anta, "On low inertia grids", Innovative controls for renewable source integration into smart energy systems (INCITE), 2017
- [8,9] Egea-Alvarez and J. Renedo, "Control of power converters in low inertia power systems: A practical approach," EES-UETP Course on low inertia power systems, Madrid, Spain, April, 2019.
- [10] Hassan Bevrana, "Virtual synchronous generators: A survey and new perspectives. Electrical Power and Energy Systems", 244-254, 2014
- [11] Egea-Alvarez, S. Fekriasl, F. Hassan, O. Gomis-Bellmunt, "Advanced vector Control for Voltage Source Converters Connected to Weak Grids," IEEE Transactions on Power Systems, vol. 30, no. 6, pp. 3072-3081, 2015
- [11] Tomas Hirst, "Britain's Renewable Energy Sector Is Surging", Business Insider, 2015
- [12] Think Grid, "WAMS: managing emerging stability risks", 2015
- [13] Alok Jha, "£75bn for UK's biggest offshore wind programme signals new era for renewables", The Guardian, 2010
- [14,15] Nordic power system, "Challenges and Opportunities for the Nordic Power System", Tech. Rep., 2016



[16] , Alice Grundy, “National Grid ESO claims world first approach to inertia, awarding £328m in contracts”, Current, Jan 2020

